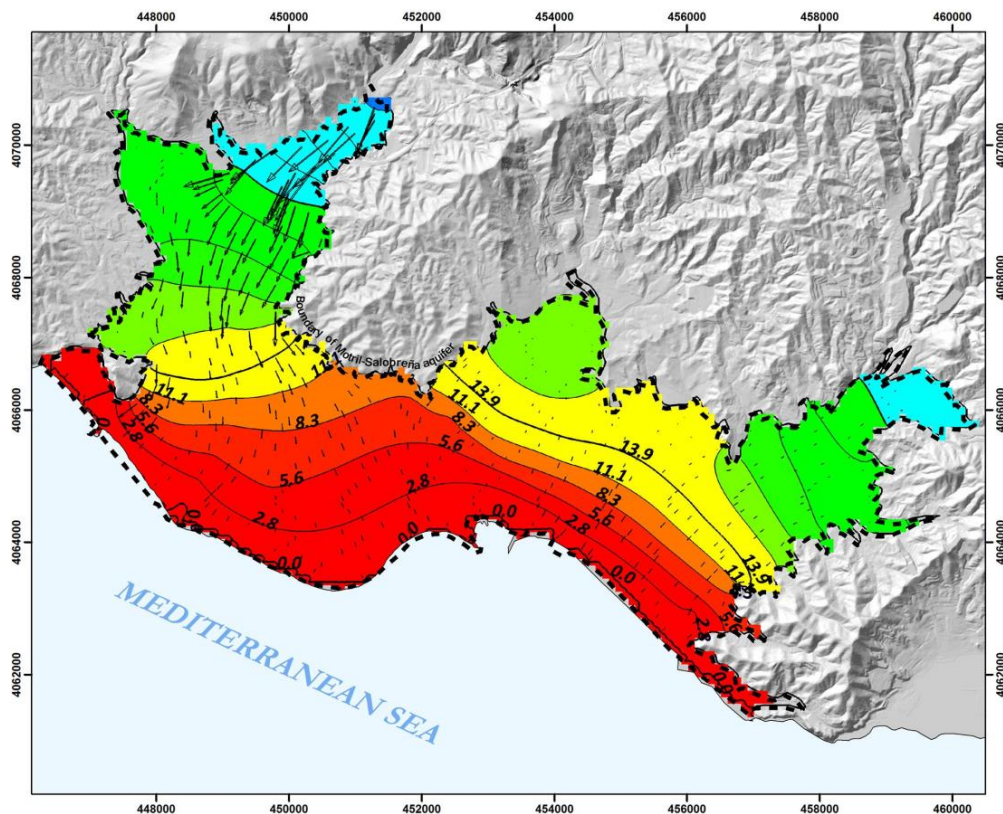# Modelling the impact of land-use change due to anthropogenic activity on hydrodynamics in an aquifer in Southern Spain

Elisabeth Døvre Ayres

UNIVERSITY OF OSLO
FACULTY OF MATHEMATICS AND NATURAL SCIENCES

Modelling the impact of land-use change due to anthropogenic activity in an aquifer in Southern Spain

Elisabeth Døvre Ayres

Master Thesis in Geosciences
Discipline: Environmental Geosciences
Department of Geosciences
Faculty of Mathematics and Natural Sciences

University of Oslo
September 2015

ABSTRACT

Land use changes increases availability of necessities, but there is also a risk of damaging or depleting natural resources. Groundwater, which is one of the most important natural resources, is dependent on having a balance between the inputs and outputs to avoid changes in the water levels. Water shortage and salt water intrusion resulting from lowered water levels, are becoming a more and more serious problem along the Mediterranean coast in southern Spain, and also in other arid places around the world. One of the few coastal aquifers in southern Spain that still do not suffer from saltwater intrusion is the aquifer in the coastal area of Motril, south of Granada, but now the aquifer is undergoing hydrodynamic changes due to a shift in land use. Using a combination of recharge calculations and a groundwater flow model the impact of land use changes on groundwater resources is studied.

Changes in land use from the 1950's to 2012 have been categorized using satellite images. The excess water from precipitation and irrigation recharging the aquifer was calculated for the different categories of as deep percolation return flow using the FAO Penman-Monteith method.

In the 1950's, sugarcane was covering 70 % of the aquifer surface. By 2007 all sugarcane fields had been replaced by other crops in need of less irrigation, like subtropical trees, vegetables and crops in greenhouses. In the same period the urban areas was also expanding. The water used for irrigation in the area of Motril have been reduced by 28 Mm^3/year from 1956 to 2012 due to land use changes. This decrease in irrigation have caused an estimated 65 % reduction in surface recharge.

Scenarios of the past have been modelled to better understand how the changes on the surface have altered the dynamics in the groundwater. Following the reductions in surface recharge, the water levels have been reduced by 1 - 2 meters in the lowlands and in vicinity of the river, while the levels in the eastern sector of the aquifer have decreased by up to 10 m. The change in water levels affects the flow in the aquifer surrounding the river, From 1959 to 2012 the stretch that is gaining water has decreased to from approximately 3000 to 1000 m.

ACKNOWLEDGEMENTS

Contents

1. INTRODUCTION

Human activity has been oriented to exploit natural resources during thousands of years, changing the environment while satisfying human necessities. Modifications to land cover and land use have been implemented to increase the availability of specific resources. One of the most evident impacts is the activity oriented to modify croplands and pastures to increase food production. Today, croplands and pastures are together covering approximately 40% of the total land surface on the planet (Foley et al. 2005; Alexandratos and Bruinsma 2012). The driving force of land use changes are usually the immediate effects they give, either if it is the increased production of food, or development promoting economic advantages (Lambin et al. 2001). The strive for economic growth is making the agriculture change to more effective and profitable crops.

Rapid increase in population and consumption, and also the use of machines and technology, have caused the changes in land use to be more widespread in the last centuries (Ramankutty and Foley 1999). The amount of irrigated land grew five-fold over 100 years, during the 20th century, giving an increase in food production which fed the growing population and stabilized the availability and prices (Rosegrant et al. 2002). The modification of nature has provided an increased availability of necessities, but also damaged and depleted natural resources. In some cases, intervention in nature causes long term consequences that are difficult to predict, like disruptions in the water balance, resource depletion, reduced flow in rivers or oxygen depletion in waters (Ramankutty and Foley 1999).

One of the most important natural resources is groundwater, being the largest source of freshwater in the hydrological cycle. More than 2 billion people depend on groundwater for their daily needs (Kemper 2004). Even if the groundwater is tied to surface supplies for recharge, the long residence time of groundwater makes it resistant to short-term droughts, giving a steady supply when there is shortage of surface water (Hiscock 2005). But excessive usage is at risk of depleting the volume of groundwater beyond the natural replenishment rate (Christopherson 2009).

Sustainable use of groundwater in aquifers needs to have a balance between the inputs and outputs, otherwise changes in the natural conditions can be triggered as

the steady drop of the water table and associated negative impacts already observed in many regions, as saltwater intrusion (Benavente 1985; Ergil 2000; Kouzana et al. 2009) or land subsidence (Syvitski et al. 2009). The main sources of natural recharge in aquifers are proceeding from precipitation and the inputs are due to the infiltration of surface water (rivers or lakes), while the outputs are the discharge to surface water, such as rivers, lakes or the sea. Anthropogenic activity adds an extra output through the pumping of groundwater for irrigation of crops and human supply, which is especially common in dry areas where precipitation is scarce and surface water is not always available (Switzman et al. 2015). In these areas, irrigation that exceeds the demand of the crop and the evaporation rate, is added as a new recharge to the aquifer. It is also very common to transport water from different catchments or sources via canals or pipe conductions. Thus, land use changes that increases the recharge can, when magnificent enough, raise the groundwater level (Dahlhaus et al. 2010). Under continuous irrigation the deep percolation has shown to raise the water table as for example in Australia Schofield and Ruprecht (1989), while water-saving irrigation technology have caused the water table to drop (Xu et al. 2010). Roberts (2012) states that one of the disadvantages when changing from a flooding to a sprinkler system is a potential decrease in storage of groundwater. Therefore, the land use is significant for how much water infiltrates into the soil.

The soil moisture increases when water is infiltrating below the surface and decreasing from evapotranspiration. When the infiltrating rate exceeds the evapotranspiration rate the soil moisture content increases until it reaches its field capacity. After that, all surplus infiltration will go to the groundwater as recharge (Hiscock 2005). The process of water infiltrating below the root zone is called deep percolation (Allen et al. 2008; Bethune et al. 2008), and depends on the crop, irrigation rate and the soil type (Macaulay and Mullen 2007; Ali 2010). It is assumed that the water that percolates below the root zone is not significantly affected by evapotranspiration, and therefore will drain downwards and ultimately reach the water table and recharge the aquifer (Delin et al. 2000).

The impact of change in land uses has been studied with the assistance of groundwater numerical models as they involve long term modifications and systems where there are multiple factors interacting, and it may be required to change both recharge

and pumping (Switzman et al. 2015), as they are often connected with each other. Krause et al. (2007) found that different scenarios of land use change only showed minor effects on the groundwater in the areas close to surface waters. At further distance from surface waters the deviations in recharge and storage were more significant, with the maximum change in water table being 4 m on a simulation of 10 years when having a smoothed annual recharge dynamic (less recharge during winter, and less groundwater loss during summer). A study conducted in the UK investigated the changes from agriculture to forestry, where the scenarios showed a decrease in recharge of up to 45 % (Zhang and Hiscock 2010). However, because of the high storage capacity of this aquifer, the effects on the groundwater levels would be limited, decreasing the water table with less than 10 % of the natural long-term variations.

In the Mediterranean coastal areas in Spain, the groundwater is an extensive source for freshwater, used to supply drinking water to the population, for agriculture and providing necessities of tourism and industry. Economical and tourist development have necessitated high water demands, and now a high percentage of the coastal aquifers struggles with saltwater intrusion (Gómez et al. 2003). This situation is caused by the combination of hot and dry summers, which increases evapotranspiration rates and therefore decreases recharge and increased pumping for high water consumption during the summer months.

One of the few coastal aquifers in southern Spain that still do not suffer from saltwater intrusion is the aquifer in the coastal area of Motril, south of Granada (Figure 1), but now the aquifer is undergoing hydrodynamic changes due to a shift in land use. In this area the production of sugarcane dates back a thousand years, to the 10th century when the Arabs introduced this crop due to the suitable climate conditions, with mild winters and high temperatures all year (Ayuntamiento de Motril 2015). The sugarcane crops were irrigated using canals with water distributed from a river (Guadalfeo River) that cross the aquifer in the western sector. The Guadalfeo River has a wide catchment, and therefore presents a yearly mean flow of 6000 L s^{-1}, that allows to provide water for irrigation. The water from the irrigation canals was then used to flood the sugarcane fields for several hours to provide the optimal conditions for the growth of this plant. However, during the last 50 years other types of crops requiring less water has replaced the sugarcane, as greenhouses and

drip irrigation for optimizing the use of water resources. Crops grown in greenhouses typically get watered by advanced systems that provide the exact amount of water required, giving a minimum water spillage going to the groundwater (Shock and Welch 2013). In addition, other modifications as the expansion of the urban areas, due to tourist activity, can be detected. Therefore, this study focus on the impact of land use change in the Motril-Salobreña aquifer on groundwater resources as well as the hydrodynamical modifications to the flow in the aquifer.

1.1. Objectives

The main goal of this study is to:

1. Quantify the land use changes in the Motril-Salobreña aquifer,

2. Estimate the recharge produced by the different irrigation techniques,

3. Implement the changes induced in the aquifer in a groundwater flow model,

4. Analyse the hydrodynamic changes in the groundwater during the last 60 years to better understand how the changes on the surface has altered the dynamics in the groundwater.

2. Area description

The Motril-Salobreña aquifer is located about 60 km south of Granada in the Andalucia region in southern Spain (Figure 1). The area of the aquifer is approximately 42 km^2, and it has three centers of population distributed on top of it. Motril, which is the largest (61171 inhabitants (2012)), is located at the north border at the central part of the aquifer. The second largest town in the area is Salobreña (12747 inhabitants (2009)), which is located at the western border, close to the coastline. Torrenueva is located in the south eastern corner of the area, and is a smaller village with a population of 2988 people (2014). Due to the comfortable climatic conditions, there have been an intense growth in tourism during the last decades, and the areas along the coastline have had an increase of urban establishment with apartment buildings, hotels and golf courses.

Figure 1: *The location of the Motril-Salobreña aquifer in southern Spain, showing the city of both Motril and Salobreña, the mountain range Sierra Nevada and the course of the river Guadalfeo. The terrain elevation is exaggerated by a factor of 2 (Satellite image from Google earth)*

2.1. Climate and Hydrology

The area of Motril has a subtropical microclimate, with warm summers and mild winters (Figure 2), having an average annual temperature of 18 °C (Ayuntamiento de Motril 2015). The area has 320 days of sun in a year, and an average precipitation of 400 mm per year (Calvache et al. 2009).
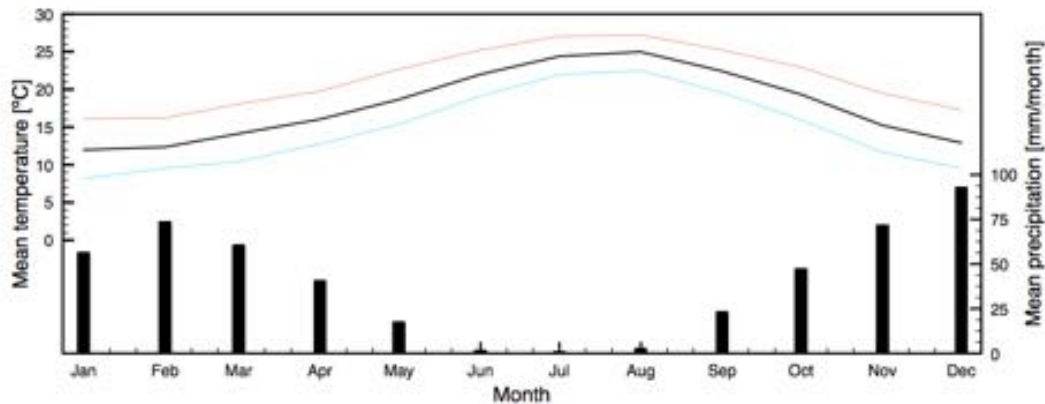
Figure 2: *The monthly mean temperature and precipitation, calculated from 2002-2013. The blue line represents the mean minimum temperature and the red line the mean maximum temperature.*

The Guadalfeo River is the main surface water body in the area, and the main source of recharge to the aquifer, and it is located in the western part of the aquifer, between Motril and Salobreña. The Guadalfeo River runs from the mountain area Sierra Nevada and down to the Mediterranean sea, crossing the Motril-Salobreña aquifer (Figure 1). The catchment extends over 1294 km^2. Despite the low rate of precipitation in the area of Motril, the precipitation in the mountain range Sierra Nevada reaches more than 1000 mm year^{-1} making the average annual precipitation for the whole catchment to be 586 mm (Calvache et al. 2009). Before 2005 the average flow rate, calculated over a 20 year period, was 6000 L s^{-1} (Duque et al. 2009). The highest flow rates takes place during the snow melting periods in Sierra Nevada and spring rains. In 2005 a dam was build upstream, to make the flow steady and avoid floods. In the 7 km track over Motril-Salobreña aquifer the river is feeding the groundwater throughout most of its course, only in the lower part, close to the sea, the aquifer is discharging into the river (Calvache et al. 2009; Duque et al. 2009) (Figure 4).

The river was channelized during the 1950's, and was earlier a natural delta with several smaller branches (Figure 3) (López 2009; Calvache et al. 2009). In addition to the natural branches of the delta, there were also man made irrigation canals distributing the water throughout the area for irrigation using gravity (Figure 5). The water of these canals is diverted from the river Guadalfeo, upstream of the aquifer. The first irrigation canal was made during the Nasrid period (13th to 15th century) (Ayuntamiento de Motril 2015), and several of the old irrigation canals are still functioning today (Calvache et al. 2009).

Figure 3: *Map of the Motril-Salobreña aquifer in 1722, showing the old river channels at the delta and the water distribution system for irrigation of the sugar cane (López 2009).*

Figure 4: *The Guadalfeo River at two locations; upstream where it enters the aquifer and downstream where it enters the Mediterranean sea.*

2.2. Geological setting

Geologically the aquifer is composed of detrital sediments carried out by the Guadalfeo River and other smaller streams coming from the nearby mountains. The sedimen-

Figure 5: *The irrigation water where it is diverted from the River Guadalfeo upstream of the aquifer, and a functioning irrigation canal passing crop fields.*

tary environment is connected to delta deposition and removement by the marine processes. The sediments in the surface of the aquifer are mainly Quaternary, while at its deepest, closest to the shore, it is up to 300 m deep with sediments of Pliocene age (Duque et al. 2007). Previous drilling of boreholes in the area showed that the sediments are ranging from coarse gravel to clay (Figure 6), with large amounts of gravel and sand in the western sector, whereas the eastern sector has higher proportions of silt and clay (Duque et al. 2007). Being a former natural delta the sediments are layered with coarser materials in the river beds and banks of prior streams, while there is bands of fine textured sediments in the old flood plains (Calvache et al. 2009) The older and deeper part of the delta consists of higher percentages of clay than the upper layers, as a result of the development of the delta.

The aquifer is located over schists, phyllites, and marble from the Paleozoic and Triassic (Duque et al. 2007) (Figure 6) seen as outcrops in the borders of the aquifer, generating steep reliefs.

2.3. Hydrogeological setting

The aquifer is defined as an unconfined detrital aquifer (Duque et al. 2009)with high hydraulic conductivity in general (1 - 300 md^{-1} (Duque et al. 2009)), with the natural changes connected to grain size variations due to different sedimentary environments. A decreasing gradient of the granulometry of the sediments from north to south and west to east (Duque et al. 2009). The geometry of the surface is limited by the outcrops of the basement hard rocks, and the depth of the aquifer is increasing from
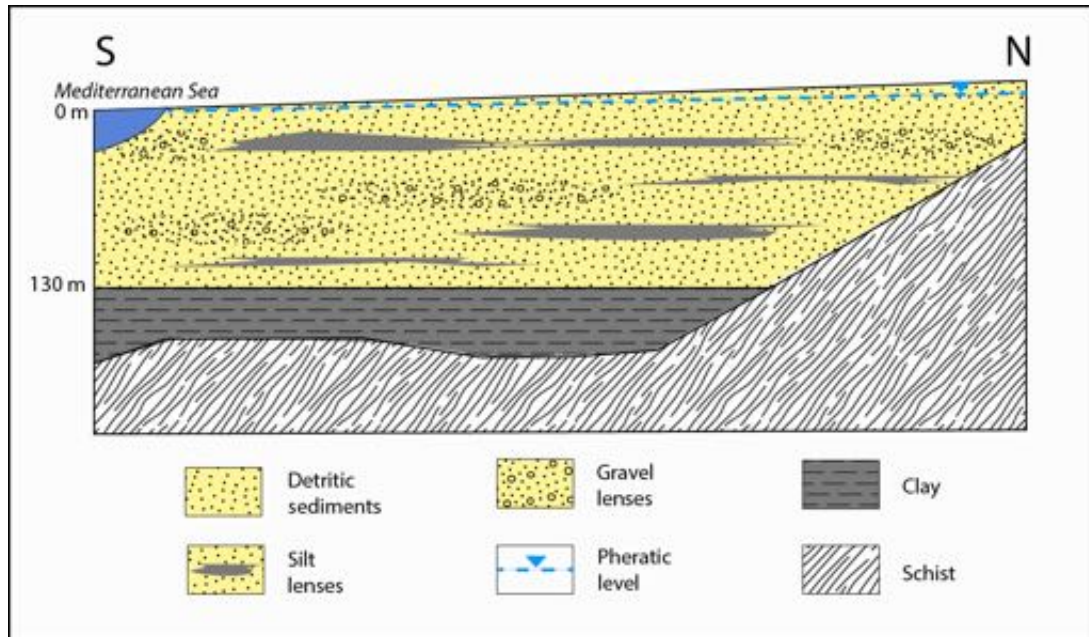
Figure 6: *A simplified illustration of the aquifer from the northern boundary with impermeable shist, to the Mediterranean Sea in the south. The aquifer consists of detrital sediments, sand with some lenses of gravel and silt/clay, placed on top of impermeable schists. The thickness of the detrital sediments is exaggerated in this figure. A layer of massive clay is present from a depth of approximately -130 m. The water table is near the aquifer surface. Modified from Calvache et al. (2009).*

north to south. The deepest points are approximately under the location of the river mouth, 250 m below the surface. Nevertheless, based on the analysis of the boreholes drilled in 2009, the sediments at a depth of more than 130 m presents a high proportion of clay, which can produce a hydraulic barrier to flow (Calvache et al. 2010) (Figure 6).

The water budget of the Motril-Salobreña aquifer has been studied by several authors (Castillo 1975; Benavente 1982; Ibánez 2005; Duque et al. 2009; Calvache et al. 2009), showing different values depending on the length of the data series used for the estimation and the methods applied. The recharge due to the infiltration from the Guadalfeo River is the most agreed on by the different studies, with 25 - 70 % of the aquifer recharge. For the irrigation and precipitation, the excess water percolating and reaching the groundwater table is more variable since it depends on the amount of precipitation during the studied period, but ranges from 15 to 47 % of the total recharge. The recharge from only precipitation is estimated to be 5 - 10 %.

The flow coming from the alluvial aquifer of Guadalfeo River, a narrow valley filled with coarse sediments, is estimated very variable depending on the method applied, from 10 to 47 % of the inputs. The contribution from a carbonate aquifer in the north is hard to estimate since the water table elevation of the carbonate and the geometry of the contact between the two aquifers is not well mapped (Duque et al. 2007), but it has been considered to account for 4 to 12 %.

In spite of being a coastal aquifer in a semiarid area, there have not been reported problems with salt water intrusion. Based on TDEM soundings and gravimetry, the zone of contact between the fresh- and saltwater is less than 500 m from the coast, and more than 150 m below the surface (Duque et al. 2006; Duque et al. 2007). This has been confirmed by recent drilling of new wells (Calvache et al. 2010).

2.4. Previous work

The area of the Motril-Salobreña aquifer has been subject to several studies and groundwater numerical models. Due to the fact that it is one of the few aquifers along the Mediterranean coast in southern Spain that still has excellent quality groundwater, as it is not affected by saltwater intrusion, monitoring the development due to human influence has been a research objective for the national and local administrations in order, to avoid a potential water quality loss in the future.

Since 2001 the aquifer has been monitored more frequent, mainly because of the building of the Rules dam upstream caused concerns about how the aquifer would be affected. Heredia et al. (2003) constructed a flow model in MODFLOW in collaboration with the Geological Survey of Spain for a study that was mapping the possible impacts of the dam (IGME 2000). The study included a constant density flow model which calculated the flow budget of an average year using data from 1982 to 1998. The model had three layers, an upper unconfined layer and an aquitard as the middle layer, making the third layer confined. Using only average values, the flow model was steady state; thus, the results obtained are only approximations to the general patterns of inputs and outputs of the system.

The first variable density flow model was made by Ibánez (2005) with the aim of simulating the dam's effect on saltwater intrusion processes. The model was made

with 12 layers, and seven zones were defined due to sedimentological knowledge to calibrate the hydraulic conductivity and specific yield. The model was simulated for the year 2001-2002 with 15 days time-step. The year was chosen as it had precipitation close to the mean of 415 mm. The predictions that were made from the simulation showed a general advance of the saline wedge in future scenarios where the inputs from the river and the irrigation were modified due to the dam effect, and the changes that this would produce in the aquifer

Calvache et al. (2009) constructed another numerical simulation of the aquifer based on the model and results by Ibánez (2005). Most of the different scenarios simulated indicated a saline advance as in the previous study, with the highest risk being at the old mouth of the Guadalfeo River, where the worst case scenario showed an advance of the saline wedge of 1200 m.

Duque et al. (2009) investigated the relations between the Guadalfeo River and the aquifer using the differences in water temperature. The study revealed that the highest infiltration rates from the river to the groundwater aquifer was present in the upper parts of the river, and then decreased further downstream. During periods with high flow rates, the infiltration was also increasing, with up to 18 % of the river flow infiltrating.

To study the different recharge sources contributing to the aquifer, Duque et al. (2011) conducted a study measuring stable isotopes, comparing the incoming water and the water in the monitoring wells. This study showed the contribution from The Guadalfeo River, the carbonate aquifer, especially in the northern sector of the aquifer, and the contribution of irrigation during summer months.

None of the previous models have been calibrated for a longer time period including the natural fluctuations due to the inter-annual climatic variations. The area of study has variable climatic characteristics, with dry and wet years with precipitation ranging from 261 mm (2004-05) to 847 mm (2010-11), but also the distribution within a year can differ from year to year. For example did the hydrological year of 2005 have the heaviest rainfall event during spring, while the next year had it in the autumn.

The previous studies have also used simplified values of deep percolation from irrigation, adding this to the infiltrated water from precipitation. The percentages

used for the deep percolation from the water supplied on the surface are highly uncertain, due to the complexity of the estimation as there are multiple parameters that have to be considered, and most importantly, due to the fact that it does not consider precipitation.

To improve the results obtained in the previous studies, the deep percolation can be calculated and implemented in a transient calibration and validation numerical model with a longer time period. This is now possible due to the long time series of data data that have been collected during the last 15 years, the availability of new data regarding the last drilling in the aquifer, and the more frequent release of aerial images.

3. Methods

A combination of methods will be used for reaching the objectives proposed, starting with analyses of aerial images to map how the prevalence of the different land uses are changing, and estimating the impact on the recharge to the aquifer. To quantify the effects of the changes, a groundwater numerical model will be implemented, considering the current conditions and how it was prior to the changes. Possible scenarios for the future based on the trends observed will also be considered and modelled. A flow chart resuming the main procedure followed in this study, connecting the available data to the applied methods and the objectives, is presented in Figure 7.
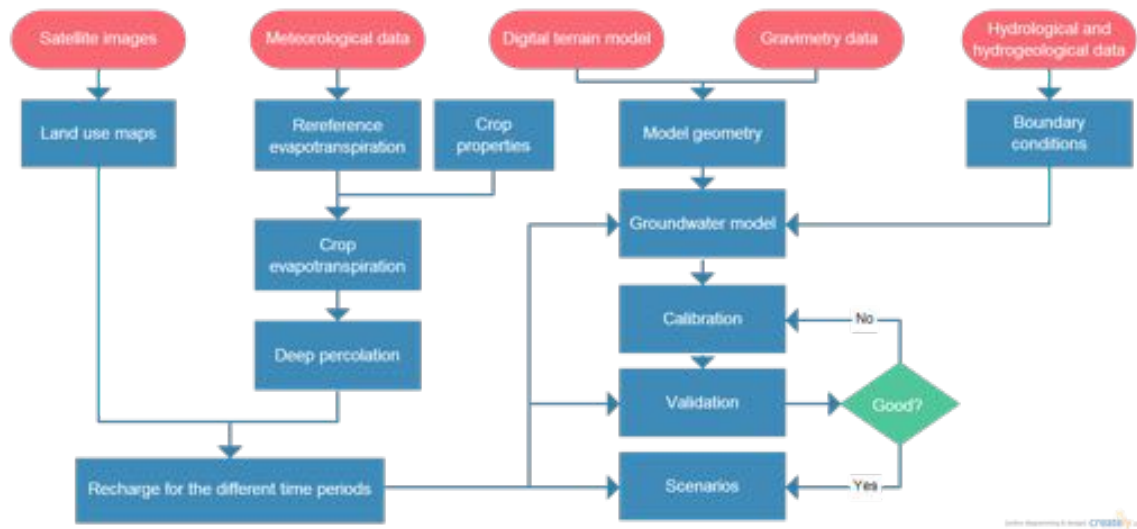
Figure 7: *Flow chart of the applied methods, using data available for the Motril-Salobreña aquifer.*

3.1. Data provided

Daily data of precipitation and temperature has been collected by the University of Granada at a weather station located east of Motril (latitude/longitude: 36,729049/-3,486419). The daily data is available from 2001 to 2014. From 1954 to 2001 there is monthly values of precipitation available. Data from October 2001 to September 2012 is shown in Figure 8.

Monthly data of the water table are available for 2001-2014 from 18 wells (Figure
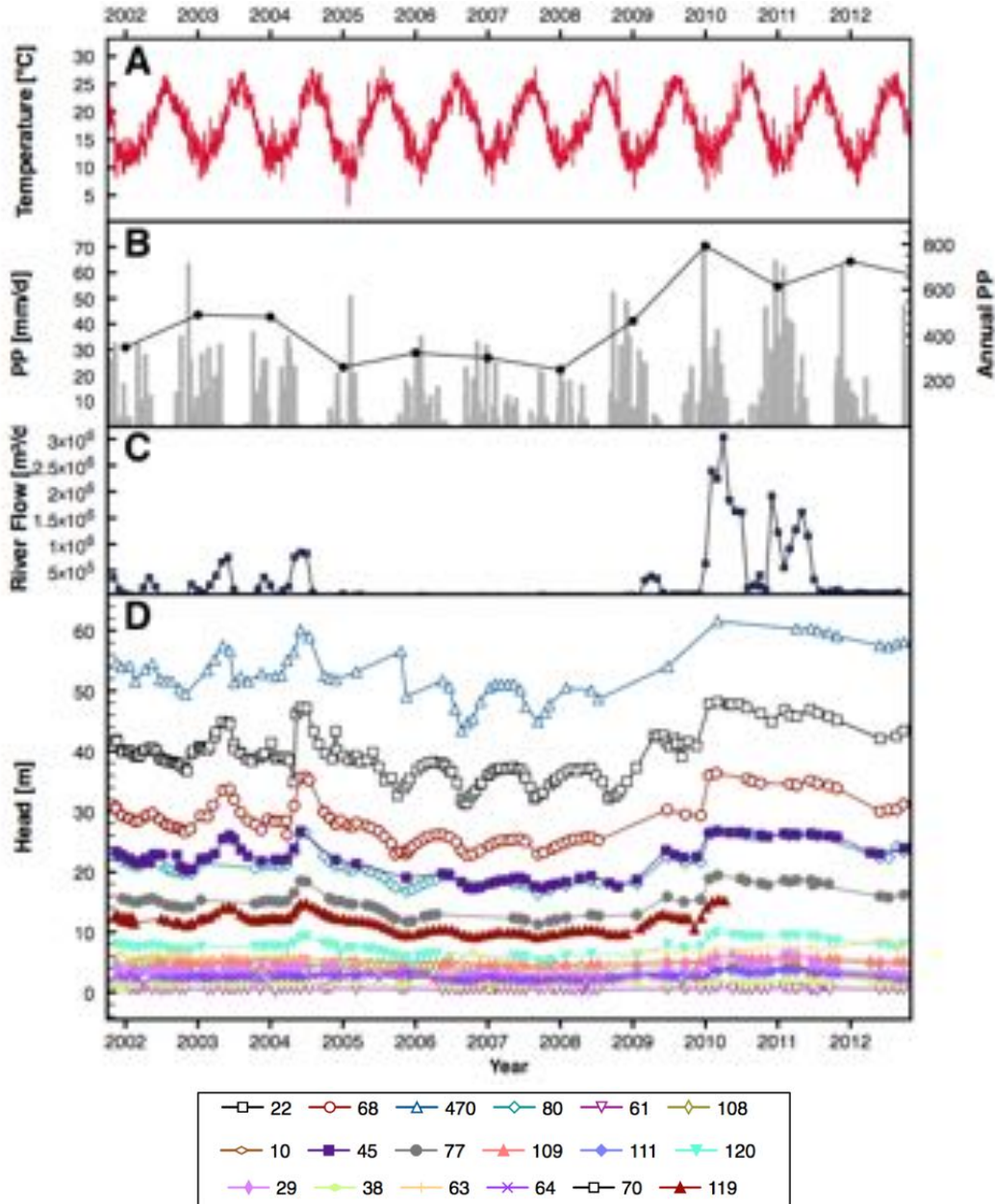
Figure 8: *Provided climatic and hydrological data of the study area from October 2001 to September 2012; A) daily temperature, B) precipitation [mm], both daily and annual (calculated for the hydrological year), C) incoming river flow [$m^3 d^{-1}$], and D) measured heads in 18 wells (Figure 9), including well 470 that is representing the carbonate aquifer and well 22 which is located in the alluvial aquifer surrounding the Guadalfeo river.*

8D) distributed around the aquifer, 8 of them close to the river Guadalfeo (Figure 9). The water table is regularly measured by the University of Granada and the

14

Geological Survey of Spain (Figure 10).
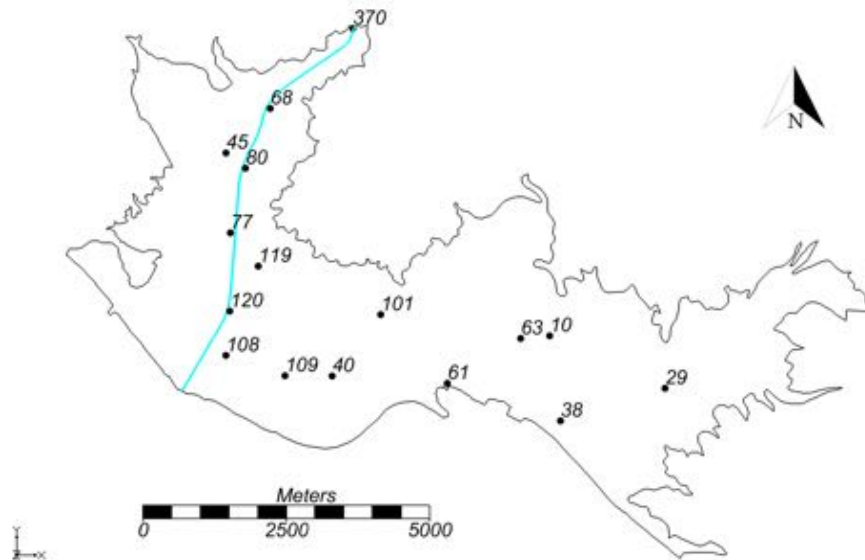
Figure 9: *The wells located on top of the aquifer, regularly monitored from 2001.*

Sporadic yearly data of pumping is available from 1973 (Castillo 1975; Benavente 1982; IGME 1999) (Figure 11). Monthly data of pumping rates from 18 wells are available from 2001-2007 showing small differences during this period.

The river flow has been monitored from 2001 to 2012 by the University of Granada, providing monthly data (Figure 8c).

Data of how much water is being used for irrigation is provided by the Office of Agriculture in Motril (OCAM 2008). Monthly irrigation rates for each type of crop is given in Table 1.

Table 1: *Monthly irrigation rates $[m^3ha^{-1}year^{-1}]$ for the different types of crops in the Motril region (OCAM 2008)*

Crop	Jan	Feb	Mar	Apr	May	Jun	Jul	Aug	Sep	Oct	Nov	Dec
Sugarcane	1340	1510	1510	0	380	760	3030	2660	1900	1510	950	950
Vegetables	1410	1460	900	380	730	700	370	580	580	1150	1180	860
Subtrop. trees	0	570	570	570	1130	1130	1130	1130	1130	570	570	0
Greenhouses	690	710	440	180	350	340	180	280	280	560	570	420

15

Figure 10: *Field measurements of water table depth.*
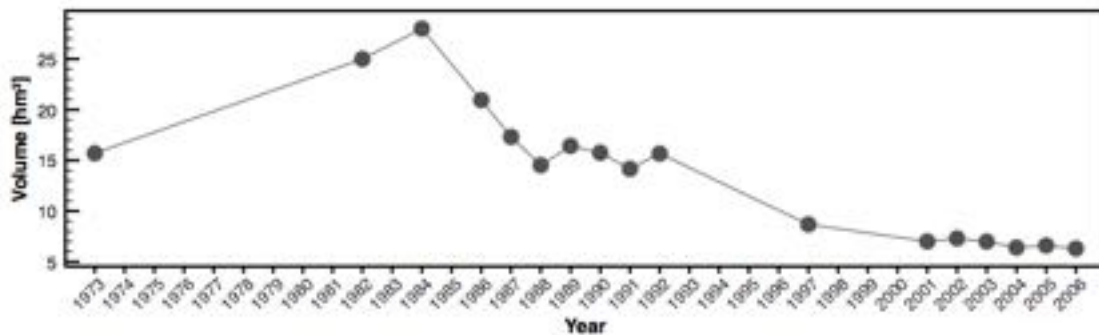
Figure 11: *Average annual pumping data from 1973 to 2006.*

3.2. Mapping the land coverage

To make the basis for the models and investigate the historical changes, the distribution of the different land uses is mapped from available aerial photographs of the area (Figure 12). The pictures used are from 1956, 1974, 1998, 2004, 2007 and 2012.

The land coverages have been divided into six categories based on their impact
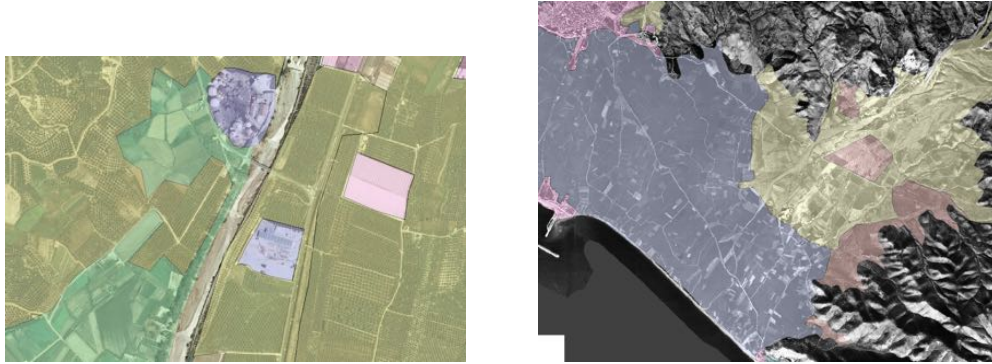
Figure 12: *The process of mapping the different landuses.*

on surface recharge; sugarcane, subtropical trees, greenhouses, grassland with no use, urban areas, and vegetables (Figure 13).

Different growth stages of the plants, depending on which season the photo was taken, and visual similarities of some categories, makes the land uses difficult to separate from each other by an automatic characterization. Therefore, manual mapping was applied, making it possible to consider which season the photo was collected. Additional field reconnaissance was done to verify the connection to the aerial photographs (Figure 13), as well as cross correlation with historical photos of the region. The extension of each coverage was quantified, and the changes for the time periods represented by each satellite image were calculated.

3.2.1. Sugarcane

Sugarcane (*Saccharum officinarum*) is widely produced for the manufacturing of sugar in tropical and subtropical regions. The stalks can grow up to 5 m tall, but more common at matured stage (after 8 months) is 2-3 m. The length of the crop cycle is varying on the climate, but for irrigated production the time until harvest is normally 12 months. (Steduto et al. 2012) The evapotranspiration rate (ET) for sugarcane is a little higher than for short grass (Inman-Bamber and McGlinchey 2003), ranging from 800 to 2000 mm depending on the climate (Steduto et al. 2012). Sugarcane have traditionally been flood irrigated, which can have as much as 40 % deep percolation (Thorburn et al. 2011; Arnold 2011).

The sugarcane have not been produced in the area of Motril after 2006, since the

(a) *Subtropical trees*

(b) *Greenhouses*

(c) *Urban areas*

(d) *Vegetables*

Figure 13: *Examples the four land uses; subtropical trees, urban areas, greenhouses and vegetables.*
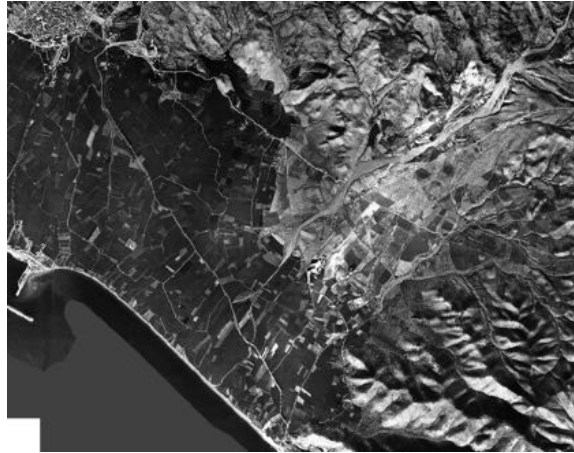
Figure 14: *An aerial image from 1956 shows the sugarcane fields as dark, almost black squares. The sugarcane is at this time grown widespread in the whole area.*

national subsidies were ended (Ayuntamiento de Motril 2015). On the older satellite images, it is noticeable by its dense and darker colour (Figure 14). Depending on the light and quality of the satellite image, it can be difficult to distinguish between sugarcane and vegetables.

3.2.2. Subtropical trees

The subtropical trees are the easiest crop to spot of the agricultural land uses, as they are characterized by a dotted pattern (Figure 13a). The subtropical trees growing in the area are mainly cherimoya (*Annona cherimola*), also called custard apple, avocado (*Persea americana*), mango (*Mangifera indica*) and a variety of citruses (Ayuntamiento de Motril 2015). An average evapotranspiration rate of these subtropical trees is used for the whole category.

The subtropical trees require aeration conditions in the soil, and therefore the irrigation system is similar to the drip method used in greenhouses, but with a higher amount, and with longer irrigation intervals. This method is considered to not produce surface runoff.

3.2.3. Vegetables

The vegetables are characterized by the long furrows they are grown in (Figure 13d) The vegetables mainly grown in the area of Motril are spinach (*Spinacia oleracea*), escarole (*Cichorium endivia 'latifolia'*), pointed cabbage (*Brassica oleracea*), celery (*Apium graveolens 'dulce'*) and potatoes (*Solanum tuberosum*) (Ayuntamiento de Motril 2015).

Furrow irrigation has low water application efficiency and high rates of deep percolation if the distribution of water is not optimally managed (Thorburn et al. 2011; Moravejalahkami et al. 2009).

3.2.4. Greenhouses

In the greenhouses (Figure 13b), dutch cucumber (*Cucumis sativus*), cherry tomatoes (*Solanum lycopersicum 'cerasiforme'*), green beans (*Phaseolus vulgaris*) and both italian and lamuyo peppers (*Capsicum annuum 'frigitello' and 'lamuyo'*) are grown (Ayuntamiento de Motril 2015).

The crops in the greenhouses are irrigated with the drip method, which is minimizing the water usage and the applied water to the plant, giving less recharge to the aquifer through deep percolation (Ayars et al. 1999; Abou Lila et al. 2013). Also, in some of the greenhouses there is an impermeable layer underneath to avoid water loss.

3.2.5. Grassland with no use

There are areas in the central parts of the aquifer which not have been cultivated in the past years, that mainly are old sugarcane fields which no longer are maintained or irrigated (Figure 15). This means that these areas have similar evapotranspiration rates as the sugarcane, but the only water recharging is proceeding from precipitation.

3.2.6. Urban areas

The category of urban areas has been mapped to include both space for transportation, low- and high-density housing (Figure 13c) and industrial areas. The urban

Figure 15: *The areas that today are not being cultivated are mainly former sugarcane fields.*

Figure 16: *One of the two small lakes in the protected wetlands in the area of Motril.*

areas are mostly covered with low-permeable surfaces, which creates higher rates of surface runoff than for the other land uses, and hence, lower groundwater recharge (Haase 2009; Gill et al. 2008).

3.2.7. Wetlands

A small protected area of wetlands (1.2 ha)are still present close to the harbour of Motril, which is located at the central part of the coastline. It consists of two small lakes surrounded by tall vegetation, and have a thriving bird life (Figure 16).

3.3. Deep percolation return flow

To calculate the deep percolation return flow from precipitation and irrigation a study of the climatic conditions in the study area and the properties of the different crop types and local irrigation techniques was accomplished.

The deep percolation return flow was calculated using the FAO Penman-Monteith method (Allen et al. 2008) by the Food and Agriculture Organization of the United Nations (FAO), which is widely used and considered as a standard (Watanabe et al. 2004). This method combines the Penman-Monteith equation of the reference evapotranspiration ET_o (Monteith 1965) with a crop coefficient factor (K_c), to obtain the actual evapotranspiration.

The FAO Penman-Monteith method requires meterological data of air temperature (mean minimum and mean maximum), solar radiation, relative humidity and wind speed. At the main weather station in Motril only the air temperature have been measured. The other data needed were collected using unofficial weather stations in the area (Windfinder 2015; Weather Undergound 2015), and by doing further calculations for missing data based on assumptions stated by Allen et al. (2008). To check the reliability of the calculations the calculated reference evapotranspiration has been compared with the results from using the Thorntwaite method (Thornthwaite 1948) and the Hargreaves potential ET equation (Hargreaves and Samani 1982). The Hargreaves equation is suggested by Allen et al. (2008) as an alternative to the Penman-Monteith method when some of the meteorological data are lacking.

3.3.1. *Reference evapotranspiration* ET_o

The Penman-Monteith reference evapotranspiration ET_o is calculated by;

$$ET_o = \frac{0.408\Delta(R_n - G) + \gamma\frac{900}{T+273}u_2(e_s - e_a)}{\Delta + \gamma(1 + 0.34u_2)} \tag{1}$$

where Δ is the slope of the saturation vapour pressure curve [kPa/°C] at temperature T; γ is the phsychometric constant [kPa/°C] which depends on the elevation; R_n is the net radiation at the crop surface [$MJm^{-2}d^{-1}$]; G is the soil heat flux density[$MJm^{-2}d^{-1}$] ; T is the daily air temperature at 2 m height [°C]; u_2 is the wind speed at 2 m height [m s^{-1}]]; e_s is the saturation vapour pressure [kPa] and e_a is the actual vapour pressure [kPa].

For daily time-steps the soil heat flux can be ignored, as it is approximately zero, and small compared to R_n (Allen et al. 2008).

The slope of the saturation vapour pressure, Δ, is calculated for the daily temperature T using the following equation (Allen et al. 2008):

$$\Delta = \frac{4098[0.6108 \times exp(\frac{17.27T}{T+237.3})]}{(T + 237.3)^2} \tag{2}$$

The net radiation at the crop surface, R_n, is the difference between the incoming short-wave radiation, R_{ns}, and the outgoing long-wave radiation, R_{nl} (Allen et al. 2008):

$$R_n = R_{ns} - R_{nl} \tag{3}$$

The radiation has not been measured at the weather station, and was therefore calculated as described by Allen et al. (2008). The potential incoming radiation is varying by time of the year and the latitude of the location, and the actual radiation is dependent on the amount of clouds and turbulence in the atmosphere. The difference between T_{min} and T_{max} is used to indicate the transparency of the atmosphere, due to the fact that clear days gives high temperatures during the days because the atmosphere is letting in more solar radiation, while the nights gets cold because less of the outgoing longwave radiation gets absorbed in the atmosphere (Allen et al. 2008).

The calculations of the extraterrestrial radiation (R_a) $[MJ\ m^{-2}\ day^{-1}]$, which is the radiation hitting the outer part of the atmosphere, is done using the latitude, daylight hours (N) and the difference in minimum and maximum temperature:

$$R_a = \frac{24(60)}{\pi} G_{sc}d_r[\omega_s sin(\varphi)sin(\delta) + cos(\varphi)cos(\delta)sin(\omega_s)] \tag{4}$$

where G_{sc} is the solar constant (0.0820 MJ m^{-2} min^{-1}); d_r is the inverse relative distance from Earth to the Sun (Equation 6); ω_s is the sunset hour angle (Equation 7) $[rad]$; φ is the latitude $[rad]$ and δ is the solar declination (Equation 8) $[rad]$.

The latitude in radians (φ) is calculated from the latitude in decimal degrees:

$$[\text{Radians}] = \frac{\pi}{180} \times [\text{decimal degrees}] \tag{5}$$

The inverse relative distance from the Earth to the Sun (d_r) is calculated with the number of the day in the year (J), where the 1st of January is day one, and the

31st of December is day 365:

$$d_r = 1 + 0.033cos\left(\frac{2\pi J}{365}\right) \tag{6}$$

The sunset hour angle (ω_s) is calculated using the latitude (φ) and the solar declination (δ):

$$\omega_s = arccos[-tan(\varphi)tan(\delta)] \tag{7}$$

where the solar declination is calculated from another equation using the number of the day (J):

$$\delta = 0.409sin\left(\frac{2\pi J}{365 - 1.39}\right) \tag{8}$$

Using the result of the previous equations (Equation 6, 7 and 8)in equation 15 gives the extraterrestrial radiation (R_a) that are used in the following equations. The solar radiation (R_s) [$MJ\ m^{-2}\ day^{-1}$], which is the radiation that is left of R_a after it has penetrated the atmosphere, being scattered and reflected, and is reaching the ground, is derived from the differences in air temperature:

$$R_s = k_{Rs}\sqrt{(T_{max} - T_{min})}R_a \tag{9}$$

where k_{Rs} is an empirical adjustment coefficient to compensate for missing calibrated ångström values (fraction of extraterrestrial radiation reaching the earth on clear-sky days), which is depending on amount of humidity and dust there is present and the solar declination. The suggested value of k_{Rs} for coastal locations is 0.19 (Allen et al. 2008).

The potential radiation reaching the ground on a cloudless day is called the clear-sky solar radiation (R_{so}), and is calculated using the elevation z [m] of the weather station:

$$R_{so} = (0.75 + 2 * 10^{-}5z)R_a \tag{10}$$

The net solar radiation (R_{ns}) [$MJ\ m^{-2}\ day^{-1}$] is the radiation hitting the surface that are not reflected, and is therefore calculated by subtracting the albedo (α):

$$R_{ns} = (1 - \alpha)R_s \tag{11}$$

where the albedo for the grass reference crop is 0.23.

When the radiation is absorbed it heats the surface, leading to the emission of longwave radiation. Some of the longwave radiation will either be absorbed by the atmosphere and emitted back to earth, or it is emitted out of the atmosphere. The net longwave radiation (R_{nl}) [$MJ\ m^{-2}\ day^{-1}$] is the difference between the longwave radiation emitted in and out from the atmosphere:

$$R_{nl} = \sigma \left[\frac{T_{max,K}^4 + T_{min,K}^4}{2} \right] (0.34 - 0.14\sqrt{e_a}) \left(1.35 \frac{R_s}{R_{so}} - 0.35 \right) \tag{12}$$

where σ is the Stefan-Boltzman contant = $4.903 * 10^-9$ MJ K^{-4} m^{-2} day^{-1}; $T_{max.K}$ is the maximum temperature during the 24-hours period (K = °C + 273.16); $T_{min,K}$ is the minimum temperature during the 24-hours period (K = °C + 273.16); e_a is the actual vapor pressure [kPa] (Equation 15) and R_s/R_{so} is the relative shortwave radiation. The results from equation 11 and 12 is then used in equation 3 to calculate the net radiation.

Continuing on calculating the other parameters needed to find the reference evapotranspiration in equation 1, the mean saturation vapor pressure e_s and the actual vapor pressure have to be calculated. The saturation vapor pressure is the pressure exerted by the water in the air when the air is saturated. The difference between the saturation vapor pressure and the actual vapor pressure, e_a, is then the capacity of evaporation to the air, also called the vapor pressure deficit.

The mean saturation vapor pressure is calculated from the air temperature:

$$e_s = \frac{e^0(T_{max}) + e^0(T_{min})}{2} \tag{13}$$

where $e_0(T)$ is the saturated vapor pressure at the air temperature T [kPa], and is calculated from:

$$e_0 = 0.6108 exp \left[\frac{17.27T}{T + 237.3} \right] \tag{14}$$

whle the actual vapor pressure, e_a, is calculated using monthly average dew temperatures, T_{dew}:

$$e_a = e^0(T_{dew}) = 0.6108 exp \left[\frac{17.27T_{dew}}{T_{dew} + 237.3} \right] \tag{15}$$

The average wind speed of the area is assumed to be 3 m/s (Windfinder 2015). The wind speed has been measured at a weather station west of Salobreña. For

normal ranges, ET_o is not highly sensitive to wind speed (Allen et al. 2008), and it is therefore assumed that this approximation is not affecting the end result significantly.

3.3.2.   Crop evapotranspiration ET_k

The crop evapotranspiration ET_c [mm d^{-1}] is the product of the reference evapotranspiration and the crop coefficient;

$$ET_c = K_c ET_o \tag{16}$$

where K_c is the crop coefficient [dimensionless], which is a factor adjusting the evapotranspiration to be valid for a specific crop with different evaporation and transpiration rate than short grass, which is the reference crop. The crop coefficient is defines as the ratio of the crop evapotranspiration over the reference evapotranspiration ($K_c = ET_c/ET_o$) (Allen et al. 2008). K_c considers the crop height, albedo of the soil surface, canopy resistance to vapor transfer and the direct evaporation from the soil.

Splitting up K_c into the crop evapotranspiration, primarily the transpiration of the crop, and the soil evapotranspiration, the evaporation of the water in the soil surface, gives:

$$ET_c = (K_{cb} + K_e)ET_0 \tag{17}$$

where K_{cb} is the basal crop coefficient and K_e is the soil evaporation coefficient.

The FAO table value of K_{cb} from Allen et al. (2008) is based on a sub-humid climate with moderate wind speed. To adjust this value to the local climate, K_{cb} is calculated with;

$$K_{cb} = K_{cb(Tab)} + [0.04(u_2 - 2) - 0.004(RH_{min} - 45)]\left(\frac{h}{3}\right)^{0.3} \tag{18}$$

where $K_{cb(Tab)}$ is the given value for K_{cbmid} or K_{cbend} if ≥ 0.45; u_2 is the average daily wind speed at 2 m height [m s^{-1}]; RH_{min} is the mean value for daily minimum relative humidity [%] and h is the mean plant height [m]. All during the plants mid or late season stage.

Average yearly data for humidity is used, RH$_{min}$ as 23 % (based on one year measurements 2014-2015) (Weather Undergound 2015).

While the crop coefficient is mainly focusing on the plant, the soil evaporation coefficient is calculated considering the soil properties;

$$K_e = K_r(K_{cmax} - K_{cb}) \leq f_{ew} K_{cmax} \tag{19}$$

where K_{cmax} is the maximum value of K_c after rainfall or irrigation, K_r is the dimensionless evaporation reduction coefficient, f_{ew} is the fraction of soil that is both wetted and exposed.

K_{cmax}

$$K_{cmax} = max\left(\left\{1.2 + [0.04(u_2 - 2) - 0.004(RH_{min} - 45)]\left(\frac{h}{3}\right)^{0.3}\right\}, \{K_{cb} + 0.05\}\right) \tag{20}$$

where h is the maximum plant height $[m]$.

The soil evaporation reduction coefficient (K_r) is a factor indicating how much water is available in the soil for evaporation. K_r is ranging from 0 - 1, with 1 meaning that the soil is wet, and 0 that the soil is dry. K_r will after precipitation or irrigation be reduced until water is added again:

$$K_r = \frac{TEW - D_{e,i-1}}{TEW - REW} \quad \text{for} \quad D_{e,i-1} > REW \tag{21}$$

where $D_{e,i-1}$ is the cumulative depth of evaporation (depletion) from the soil surface layer at the end of the previous day (day$_{i-1}$) $[mm]$; TEW is the maximum cumulative depth of evaporation (depletion) from the soil surface layer when K$_r$ = 0 $[mm]$ (Equation 22) and REW is the cumulative depth of evaporation (depletion) at the end of the initial stage $[mm]$.

REW (Readily evaporable water) is the maximum depth of water that can be evaporated from the topsoil layer before the evaporation rate starts reducing. Typical values of REW given by Allen et al. (2008) ranges from 5 to 12 mm, with the highest values for finer materials.

TEW, the total evaporable water $[mm]$, which is the maximum depth that water can be evaporated after the soil surface has been completely wetted ($K_r = 1$), is calculated using soil properties:

$$TEW = 1000(\theta_{FC} - 0.5\theta_{WP})Z_e \tag{22}$$

27

where θ_{FC} is the soil water content at field capacity [m³ m⁻³]; θ_{WP} is the soil water content at wilting point [m³ m⁻³] and Z_e is the depth of surface soil layer that is subject to evaporation [m]. The recommended value for Z_e is 0.10-0.15 when unknown (Allen et al. 2008).

The fraction of exposed and wetted soil (f_{ew}) is indicating how much of the surface in the field that are subject to evaporation. The part of the soil that is not wetted or is covered by vegetation is assumed to have a lower evaporation rate. Since f_{ew} is either the soil exposed, or the soil wetted, it is calculated as:

$$f_{ew} = min(1 - f_c, f_w) \tag{23}$$

where $1 - f_c$ is the average exposed soil fraction and f_w is the average fraction of soil wetted by irrigation or precipitation.
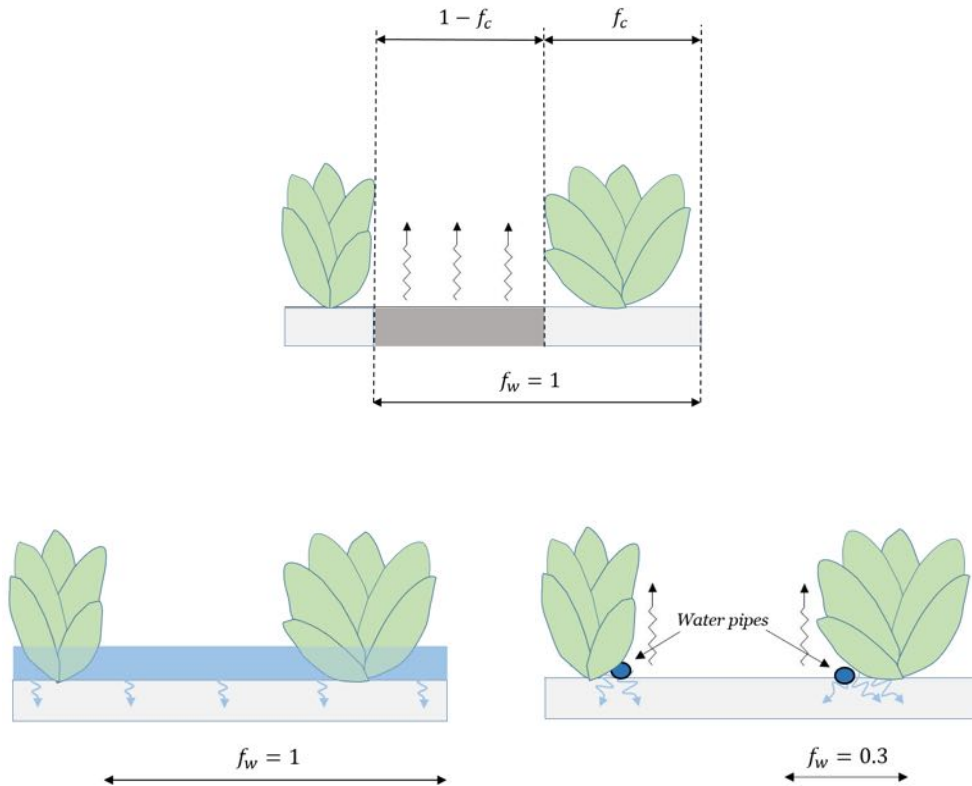

Figure 17: *The wetting fraction coefficient (f_w) and the ground surface coverage (f_c). Flooding covering the whole field is giving a wetting fraction of $f_w = 1$, while methods distributing smaller amounts of water, like the drip method, gives a smaller wetting fraction. Modified from Allen et al. (2008), figure 39.*

The parameters used in the calculations of the crop evapotranspiration are given in Table 2. Most of the top soil in the area is in the range of sandy clay loam to sandy loam (Pleguezuelo et al. 2011; IGN 2006). The values chosen for the hydraulic conductivity and porosity for sandy clay loam in this aquifer is taken from the typical values and the standard deviation presented in Dingman (2002) and Allen et al. (2008).

Table 2: *Properties of the top soil used in the Penman-Monteith calculations, based on Dingman (2002) and Allen et al. (2008).*

Parameter	Top soil
Soil texture	Sandy clay lome
θ_{FC} [$m^3 m^{-3}$]	0.2
θ_{WP} [$m^3\ m^{-3}$]	0.07
Z_e [m]	710
REW [mm]	8
TEW [mm] $= 1000(\theta_{FC} - 0.5\theta_{WP})Z_e$	16.5
u_2 [$m\ s^{-1}$]	3

Table 3: *Parameters of the different types of crops used in the Penman-Monteith calculations, based on Allen et al. (2008). * Weighted arithmetic mean of the crops for each category, and for the periods of growing (Equation 24). ** Surface runoff only when precipitation or irrigation exceeds 30 mm d^{-1}.*

Parameter	Sugarcane	Vegetables	Subtropical trees	Greenhouses	Urban areas	Wetlands	No land use
K_{cb-ini}	0.15	0.15	0.50 - 0.75	0.15	-	1.05	0.88
K_{cb-mid}	1.20	0.90 - 1.10	0.75 - 1.10	0.95 - 1.10	-	1.05	0.88
K_{cb-end}	0.70	0.65 - 0.90	0.70 - 0.80	0.60 - 0.80	-	1.05	0.88
K_{cb}*	0.88	0.75	0.78	0.73	-	1.05	0.88
f_w [-/-]	1.0	0.8	0.5	0.3	1.0	1.0	1.0
Surface RO** [%]	20	20	20	0	30	0	20
Interval [$days$]	7	7	2	1	-	-	-
Max plant height [h]	3	0.3	4	0.3	-	3	2

The parameters used for calculating the basal crop coefficient (K_{cb}) are presented in Table 3. The stage of the crops have been defined as one parameter that can modify the evapotranspiration rate, since the crop is using different amounts of water at different stages. To simplify the calculations without knowing the exact stage of the crop for each month, an average table value crop coefficient ($K_{cb(tab)}$) is used for the different categories. Based on the description of the length of each crop stage in Allen et al. (2008), The weighted arithmetic mean value for each crop category has been calculated as:

$$K_{cb} = \frac{K_{cbini} + 2 \times K_{cbmid} + 2 \times K_{cbend}}{5} \tag{24}$$

it is assumed that the initial stage is one part long, while both the mid and the final stage is two parts long. The crops in the area are having their mid stage at different times, so in total the an average value is assumed to be representative for the whole area at all times. For this estimation it was required to know which specific crop was considered in each category. The FAO reference values do not include all the crops present in the study area (crops mentioned in section 3.2), but the primary crops that have given reference values was used for the calculations of K_{cb}. The primary crops in greenhouses used for the calculations are cucumber and tomatoes. For the vegetables category the crops considered was; spinach, celery, cabbage and potatoes; and for the subtropical trees; avocado, stone fruit trees and citrus.

The fraction of wetted soil surface f_w (Figure 17) is chosen based on the typical values from Allen (2008) that are given for each irrigation technique. For vegetables, which are watered using furrow irrigation, a value of 0.8 is chosen, for the subtropical trees with a mixed technique a value of 0.5 was chosen, and for the crops in greenhouses the fraction of wetted soil is only 0.3. For the flooding of sugarcane a value of 1.0 is chosen, even if this is furrow irrigation. When watering sugarcane in this area the whole field is being flooded covering all the soil, and therefore the wetting factor is 1.0. For precipitation, the factor is also 1.0, as the water is also distributed evenly on the whole surface.

Flood irrigation is totally submerging the furrows in water for several hours (Mundy et al. 2003), making the surface runoff be approximate 10 % - 20 % or higher (Mundy et al. 2003; Austin et al. 1996). When there is irrigation or precipitation that exceeds 30 mm d^{-1}, the surface runoff is assumed to be 20 % for fields and unused land, and 30 % for the urban areas, assuming a 35 % to 50 % impervious surface (FISRWG 1998).

The irrigation of sugarcane and vegetables is set to have an interval of seven days (weekly), while subtropical trees which are irrigated more often are set to have an interval of two days. In greenhouses the irrigation is continuous, and is calculated with daily intervals (Shock and Welch 2013; Abou Lila et al. 2013).

3.3.3. Thornthwaite and Hargreaves equation

To validate the calculations done it section 3.3.1, the potential evapotranspiration rate for the area has also been calculated using the Thorntwaite and the Hargreaves equation to compare with the FAO reference evapotranspiration rate. The potential evapotranspiration rate considers infinitely water availability.

The Thornthwaite potential evapotranspiration (ET_p) (Thornthwaite 1948) calculates monthly evapotranspiration rate based on the average daily temperatures:

$$ET_p = 1.6 \left(\frac{L}{12}\right) \left(\frac{N}{30}\right) \left(\frac{10T_a}{I}\right)^\alpha \tag{25}$$

where L is the monthly average sun hours; N is the number of days in the month; T_a is the average daily temperature [°C]; I is the heat index calculated from the monthly mean temperatures $I = \sum\limits_{i=1}^{1} 2\left(\frac{T_{ai}}{5}\right)^{1.514}$ and α is calculated by $\alpha = (6.75 \times 10^{-7})I^3 - (7.71 \times 10^{-5})I^2 + (1.792 \times 10^{-2})I + 0.49239$.

Hidrobas 3.0 (Alonso-Martinez et al. 2000) have been used to calculate the monthly potential evapotranspiration according to the Thornthwaite equation.

The Hargreaves ET_p (Hargreaves and Samani 1982) is calculated by the following equation based on the difference in maximum and minimum temperature:

$$ET_{HG} = 0.0135(T_{mean} + 17.8)K_r(T_{max} - T_{min})^{0.5}R_a \tag{26}$$

The extraterrestrial radiation (R_a) is calculated as in section 3.3.1, and expressed as mm d^{-1}.

3.4. Modelling framework

To simulate the influence of a change in vertical recharge on the groundwater dynamics, a 2D numerical groundwater model was developed to simulate the transient groundwater flow. GMS (Groundwater Modeling system; Aquaveo 2015), which is a graphic interface for using the USGS groundwater flow model MODFLOW (Harbaugh 2005), was used for the simulation. MODFLOW is solving the following equation, based on Darcy's law, of two-dimensional flow through a porous media:

$$\frac{\delta}{\delta x}\left(K_x h\frac{\delta h}{\delta x}\right) + \frac{\delta}{\delta y}\left(K_y h\frac{\delta h}{\delta y}\right) + N = S_y\frac{\delta h}{\delta t} \tag{27}$$

where K_x and K_y are the hydraulic conductivity in the x and y direction, h is the potentiometric head (or aquifer depth), N is the recharge [m^3/d], S_y is the specific yield of the porous material and t is time.

3.4.1. Boundary Conditions

The conceptual model is based on the outline of the aquifer and the boundaries are based on the geological and hydrological conditions (Figure 18).
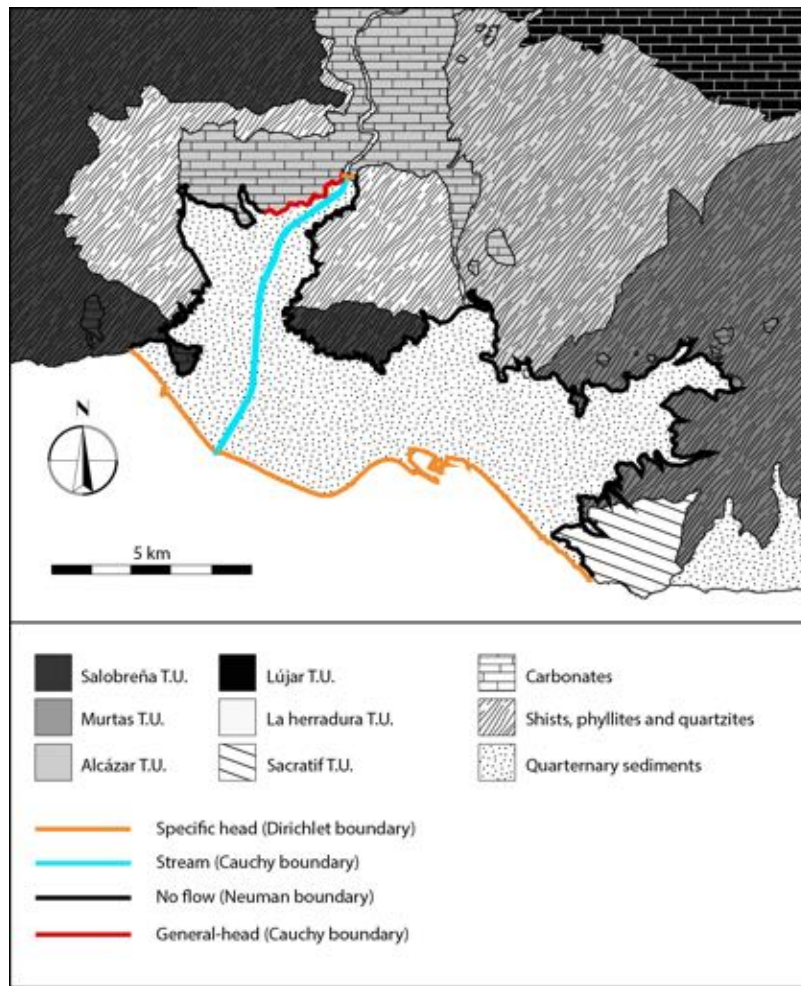

Figure 18: *A geological map of the area with the different boundaries marked. The surrounding shists from the different tectonic units (T.U.) are assumed to be impermeable. Geological map based on MAGNA 50 (2nd Series) - Geological Map of Spain 1:50.000, modified from Duque et al. (2007).*

The alluvial valley where the Guadalfeo River is entering the aquifer at the point

furthest to the north is hydraulically connected with the Motril-Salobreña aquifer (Figure 19). The inflow from these sediments is represented as a Dirichlet boundary, a specific head boundary with varying head.

The area west of the river has flow from the carbonates, where it is in contact with the detrital aquifer (Figure 19). This boundary was established as a Cauchy boundary (Harbaugh et al. 2000), where the flow will depend on the difference in heads of the carbonate and the detrital aquifer, and the connectivity between both units. The boundary extends for almost 2.5 km, but the water table in this aquifer is only measured in one well located furthest to the north. A decrease of the water table along this contact is expected, and hence, based on the natural slope of the terrain, the water table was decreased by 5 % along the border.
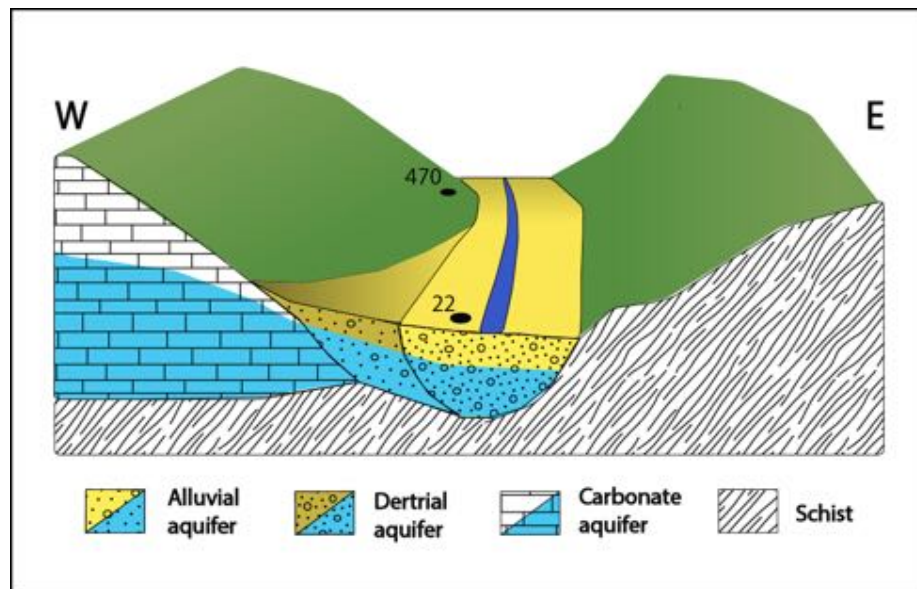

Figure 19: *The northern area of the aquifer where the river is entering the aquifer, together with flow through the alluvial aquifer surrounding the river, and water from the adjacent carbonate outcrops enters the detrital aquifer. Well 470 is placed in the carbonates, while well 22 is located in the alluvial aquifer, close to the river. Modified from Duque et al. (2011).*

The contact between the aquifer and the Mediterranean Sea in the south is represented with a Dirichlet boundary condition with the mean elevation of the sea (0 m). The rest of the aquifer is delimited by surrounding low permeable schist that is represented with a no-flow boundary.

The Guadalfeo River was simulated using Cauchy boundary conditions with the

Streamflow-Routing (SFR2) package (Niswonger and Prudic 2005). This package allows to have extreme changes in flow, even a dry channel if the environmental conditions are promoting it. In the Guadalfeo River, especially during summer, the river channel can get totally dry, and even if there is a small amount of flow in the northern sector, this infiltrates or evaporates before reaching the river mouth. The river is represented with eight stream segments, with their elevation taken from a topographic map. Based on field measurements, the stream channel was simplified to be symmetric, with the depth and width constant for all three segments, respectively 3.0 and 20.0 m. The roughness of the riverbed is assumes to be 0.05, based on comparison with the visual guide of river roughness characteristics (Barnes 1967). The conductance in the river is assigned using the thickness (b) and hydraulic conductivity (K) in the riverbed (Harbaugh 2005):

$$C_b = K\frac{A}{b} \tag{28}$$

where A is the area of the riverbed. Both the thickness and the hydraulic conductivity are unknown parameters, and are part of the calibration process.

The pumping has been established based on the monthly groundwater withdrawals in each of the wells (Neumann boundary condition) . The recharge has been established as a Neumann boundary condition with specific flow, adding the flux resulting from adding precipitation and irrigation and removing evapotranspiration and soil retention for each of the land cover categories.

3.4.2. Aquifer Geometry

The model consists of 4563 100×100 m grid cells with varying thickness. The top elevation of the aquifer is obtained from a digital terrain model (DTM) with spacial resolution of 10x10 m from the Spanish Geographical Institute (IGN n.d.).

The bottom elevation was interpolated from previous geophysical data (Duque et al. 2009) together with placed points around the border of the aquifer (Figure 20). The maximum depth of the aquifer was set to be at 130 m below sea level, due to presence of massive clay. The clay is assumed to be a hydrogeological barrier because of its low permeability.

Due to the high increase of elevation at the border of the aquifer because of the steep topography, the interpolated surface representing the bottom of the aquifer had to be corrected. The correction consisted of adding points around the border of the aquifer to keep the elevation of the bottom of the aquifer below the topographic surface, as well as the removal of points that induced errors. The highest elevation of the bottom was set to be -10 m.a.s.l. This is an artificial chosen number to make sure all the cells made flow possible, but since the saturated zones in these areas are thin compared to the rest of the aquifer, it is assumed that it will not influence the results in a great extent. Natural neighbor was chosen as the interpolation method of the points, after observing the most realistic result and with least errors of higher elevation of the bottom of the aquifer than the topographic surface.

In the areas where the aquifer extension was one single cell, the cell was as inactivated (Figure 21) to avoid converging errors. As the surface is reduced, this will not be influencing the final result.

3.5.   Model Calibration and validation

The data from October 2001 to September 2007 are used for calibrating, while the data from October 2007 to September 2012 are used for validating the model. Calibration of the groundwater model is based on the comparison of the simulated and observed groundwater table stages after the modification of the parameters of the model and the distribution of them. The model was initially calibrated in steady state with average values for recharge and stream flow to reach starting values of hydraulic conductivity and S. After that the model was calibrated in transient regime with monthly stress periods, and daily time steps. The parameters calibrated were the horizontal hydraulic conductivity, the specific yield (S_y), the conductance of the carbonate aquifer border and the conductance of the riverbed.

The horizontal hydraulic conductivity was calibrated because the sediments observed in the lithological columns were changing from clay, silt and sand to gravel in short distances due to the mixed sedimentological environments, and it was difficult to establish a pattern based only on the information from the boreholes. In addition, since the model is in 2D, the hydraulic conductivity of each cell is rep-
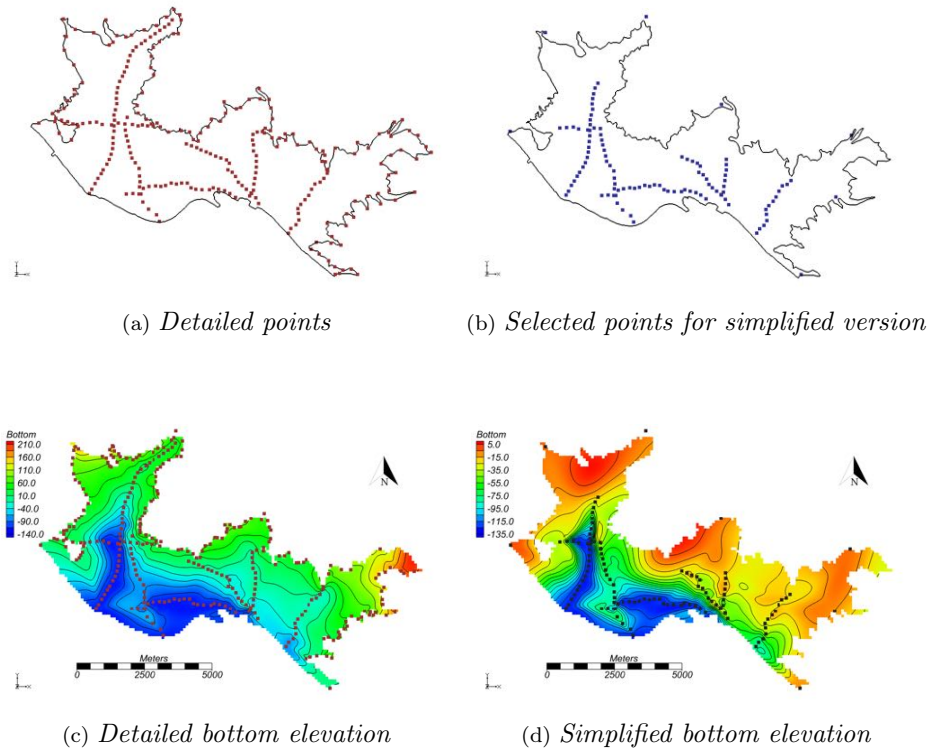
(a) *Detailed points*

(b) *Selected points for simplified version*

(c) *Detailed bottom elevation*

(d) *Simplified bottom elevation*

Figure 20: *(a and b)The points for making the bottom elevation in both the original detailed version and the simplified bottom. In the simplified version the points in the upper corners represent the highest points with an elevation of -10 meters. (c) Detailed bottom elevation interpolated from the dataset with detailed bottom elevation points. (d) A simplified bottom elevation with a lower maximum elevation. The lower part of the aquifer has the same detail level for both versions.*
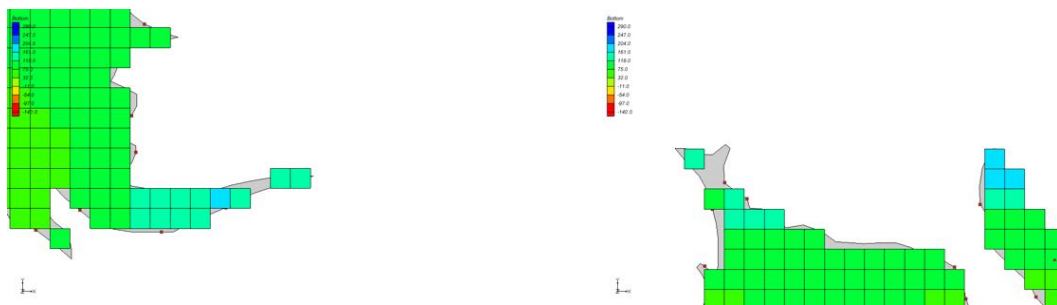

Figure 21: *Cells that are not connected with flow are defined as inactive.*

resenting an average of the hydraulic conductivity at different depths. Considering this, the calibration of hydraulic conductivity was done using automated parameter estimation (PEST) with the pilot points technique (Doherty 2003). The pilot points were placed between the observation points to make sure the pilot point always has two or more heads to calibrate from (Figure 22). PEST adjusts the model parameters by minimizing the difference between the modelled value and the corresponding measurement, using a non-linear estimation technique. This technique is known as the Gauss-Marqwardt-Levenberg method (Doherty 1998). Pilot points considers a gradual change of the variables between the defined pilot points, in contrast to zonation-method which creates sudden changes from one cell to another (Doherty 2003).

Since the hydraulic conductivity in this model is a vertical average, and the sediments that compose the aquifer are well known, gradual changes of hydraulic conductivity is the most likely possibility.

For the calibration of the specific yield a zonation was defined based on analysis of boreholes and previous data (Calvache et al. 2009), and the final values for each zone calibrated using PEST (Figure 23).

Flow through the stream bed and through the border between the carbonate and the detrital aquifer are connected with the conductance between the riverbed . The riverbed conductance was calibrated as a ratio of the hydraulic conductivity of the riverbed and the thickness (Equation 28), since detailed knowledge about both are lacking. Keeping the riverbed thickness at 1 meter for the whole calibration process, the conductance was calibrated changing the hydraulic conductivity. This was accomplished both with PEST and manually by trial and error to fit the model results to the observed variations.

The calibration of the riverbed thickness/permeability of the river and the leakage from the carbonate aquifer border was calibrated manually by the trial-and-error method.

As shown in the flow chart of the methods (Figure 7), the results from the calibration were used together with the data sets for the period from October 2007 to September 2012 in order to validate the results. The validation process showed that the calibration can produce different sets of data that had a different effect in
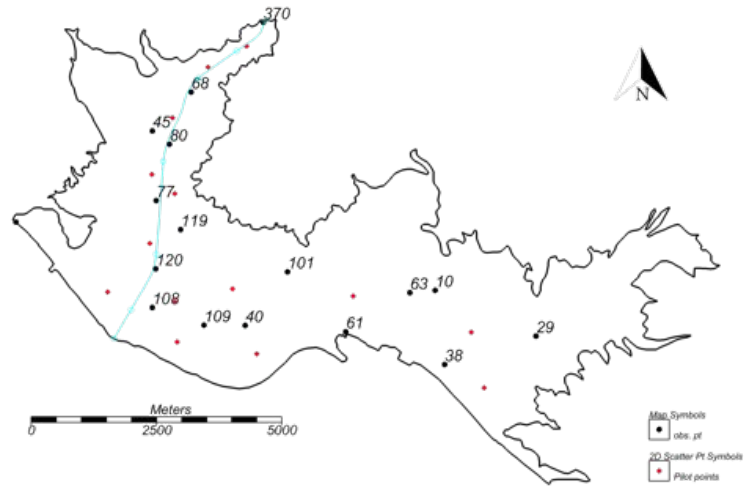
Figure 22: *The observation wells (circles) and the pilot points used for calibration of the hydraulic conductivity (squares).*
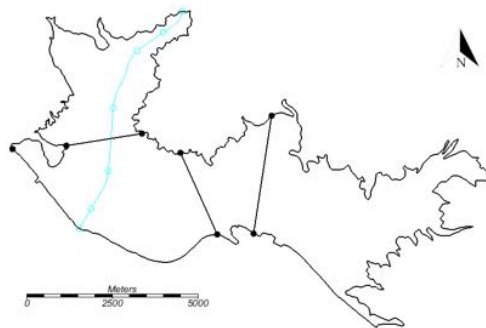

Figure 23: *The aquifer divided into zones to calibrate the specific yield.*

the results. It was required to obtain six calibrated sets until obtaining a result that showed an acceptable validation result. During this process the specific yield, the conductance of the riverbed and the hydraulic conductivity were modified until reaching a solution that could be validated.

3.6. Generation of scenarios

Two scenarios were considered to study the changes related to the recharge in the aquifer and the hydrodynamic changes. Model 1 is representing the time period when the sugarcane was covering the aquifer, as the irrigation system by flooding is expected to affect to the groundwater dynamic, this is corresponding to the 1950's. Model 2 represents the 1970's, which was a transitional period when subtropical trees and greenhouses where started to be introduced in the area, in addition to an initial expansion of the urbanized areas.

The data available for the earlier years are not as detailed as from after 2000, so to make sure that the different data inputs correspond, the scenarios are modelled using data from years after 2000 with similar precipitation. Since the other data, both heads in the carbonate and alluvial aquifer, flow in the river and deep percolation, are products of the precipitation, it is assumed that the whole dataset is representative for the period with similar precipitation. Each scenario includes a dataset with fluctuating precipitation similar to the actual fluctuations of the period (Figure 24 and Table 4).
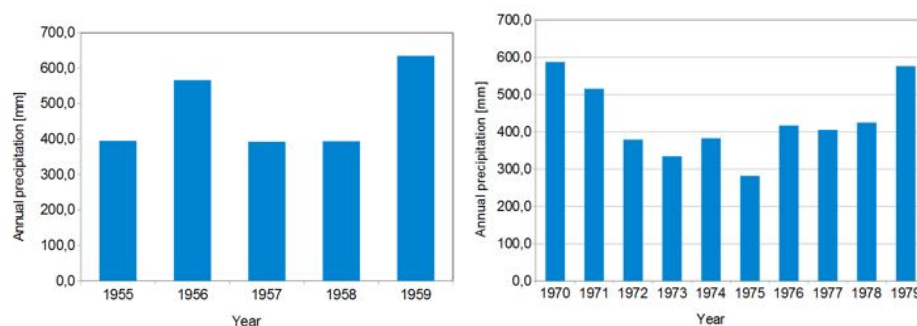

Figure 24: *The annual precipitation of the hydrological years in the 1950's and the 1970's.*

The earliest estimated pumping data available is for 1973 (Castillo 1975), and is a

Table 4: *The years considered in the simulations, with the respective precipitation, together with the corresponding dataset.*

MODEL 1				MODEL 2			
Simulated year	Precipitation sim year	Dataset year	Precipitation data year	Simulated year	Precipitation sim year	Dataset year	Precipitation data year
1954-55	395.2	2001-02	348	1970-71	516	2002-03	493
1955-56	566.6	2002-03	493	1971-72	379	2001-02	348
1956-57	392.6	2001-02	348	1972-73	335	2001-02	348
1957-58	393.9	2001-02	348	1973-74	383	2001-02	348
1958-59	634.7	2011-12	724	1974-75	282	2004-05	261
1959-60	532.6	2002-03	493	1975-76	417	2008-09	463
				1976-77	405	2001-02	348
				1977-78	425	2008-09	463
				1978-79	576	2002-03	493
				1979-60	363	2001-02	348

rate of 15.7 hm^3/year. This is an estimate on the total amount of water being pumped up from the whole area, and it was divided on all the 18 present wells proportional to which wells withdraws the most water today, since information on which wells that were actively used during the scenario periods were not available.

4. RESULTS

4.1. Historic land use change

The land use maps made from the satellite images (Figure 25) shows how the production of sugarcane decreased from the 1950's, when it was occupying most of the surface. During the 70's other crops were introduced, and areas with subtropical trees and greenhouses began spreading in the eastern sector. Around the turn of the century the sugarcane was still being produced in the lower areas surrounding the Guadalfeo River, while vegetables had replaced most of the sugarcane fields elsewhere. The northwestern area was at this time mainly cultivated with subtropical trees. For the last 10 years the area has been characterized with a more diverse land use, with greenhouses spread all over the aquifer, while the sugarcane is no longer being grown. During all the periods the urban areas were extending in the proximity of the main villages in addition to new establishments along the coast.

In 1956, the land use was distributed as 70 % sugarcane and 22 % uncultivated land, while only 4 % was considered as urban area and 3 % as subtropical trees (Figure 26). In 1974, greenhouses had started to replace sugarcane fields, counting for 4 % of the land cover. The urban areas were also growing, covering 14 % of the area in 1974. The amount of sugarcane had been reduced to cover 60 % and the unused land to 4 %.

From 1974 to 1998 the sugarcane was further reduced to 18 %, while the amount of unused land was stable only having a minor increase to 6 %. Urban areas had a slight increase to 15 %, while the amount of greenhouses and subtropical trees had doubled to cover 9 % and 30 % respectively of the total land area. Vegetable crops had in 1998 replaced approximately a third of the previous sugarcane fields, and were covering 19 % of the area.

From 1998 to 2004 greenhouses had the largest increase (from covering 9 % to 14 %), replacing some of the vegetable crops and remaining sugarcane fields that both had a small decrease from 1998. The vegetable crops were after this decrease covering 18 % and the sugarcane fields were covering 14 % of the land area. In 2007 sugarcane was no longer being produced in the area, however, vegetables had an increase to 21

%, urban areas to 20 %, and areas with no land use to 13 %, while the amount of greenhouses was stable, with only a minor decrease that might be due to measuring error.

The land use was drastically changing from 1956 to 2007, when there is no sugar cane fields left in the area. In 2012 the land use is distributed as 32 % subtropical
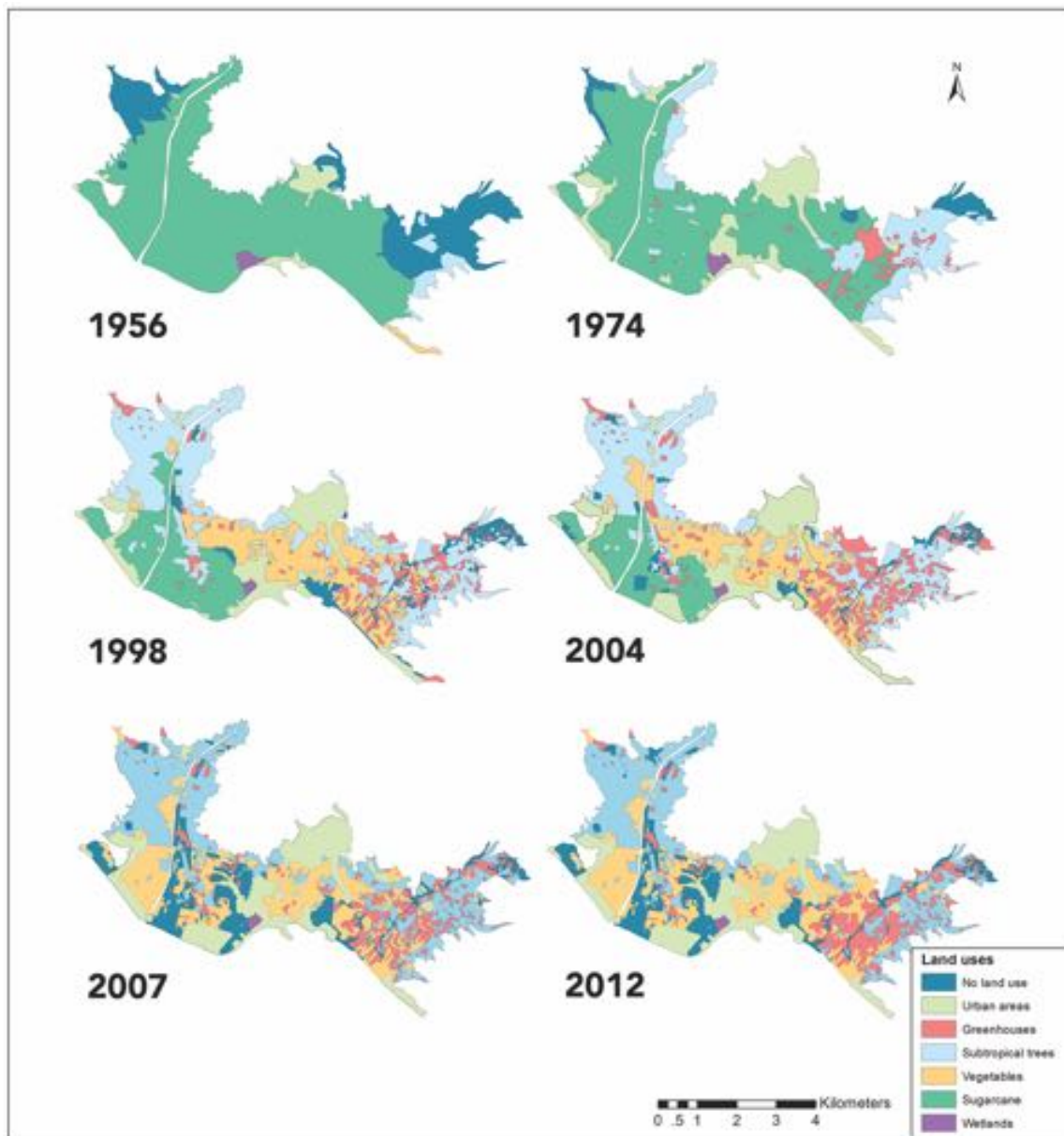

Figure 25: *Maps illustrating the land uses in the area of Motril from 1956 to 2012.*
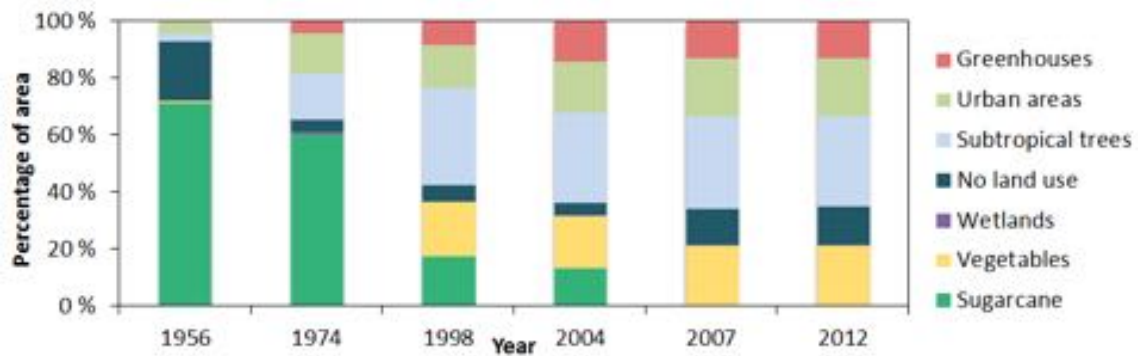
Figure 26: *The distribution of the different land use categories in the area of Motril, from 1956 to 2012.*

trees, 13 % greenhouses, 21 % vegetables, 13 % unused land and 20 % was considered as urban area.

For the whole period, from 1956 to 2012, the sugarcane had a drastic reduction, while land uses like vegetable crops, greenhouses and urban areas increased (Figure 27). Areas with no land use decreased in total, but the sudden stop in the sugarcane production left several fields unirrigated.
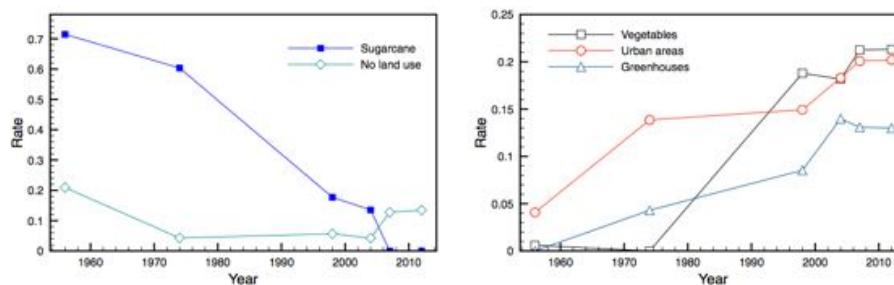
Figure 27: *The sugarcane is decreasing from covering 70 % of the area in 1956 to no longer being present in 2007. As the sugarcane, the areas with no land use is decreasing from the 50's to the 70's, but after that it increase slightly. At the same time the areas with vegetables and greenhouses and urban areas are increasing. From 2007 to 2012 the increase of vegetables and urban areas flattens out, while the amount of greenhouses have a small decrease from 2004.*

Based on the water usage for each crop type provided from the Office of Agriculture in Motril, previously given in Table 1, the changes in land use have caused a decrease in the total water usage for irrigation by approximately 50 % from 1956 to 2012 (Figure 28).

43

Figure 28: *The amount of water used for irrigation of sugarcane, vegetables, subtropical trees and plants in greenhouses from 1956 to 2012.*

4.2. Recharge

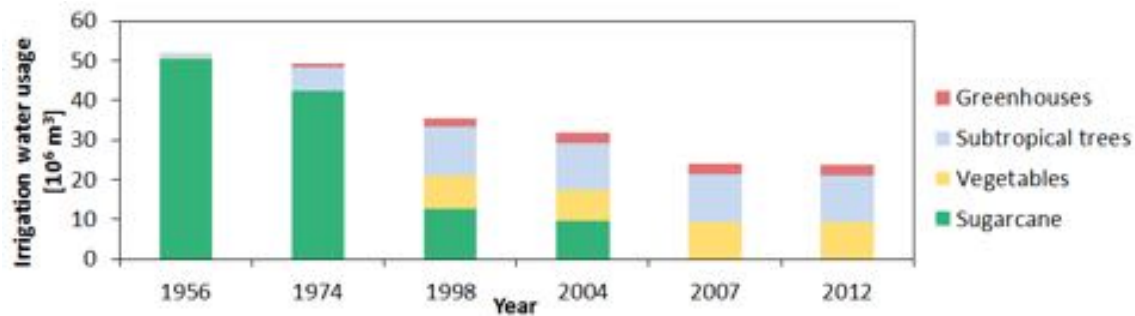The calculations of recharge from the different crops from 2001 to 2012 resulted in an average deep percolation from irrigation and precipitation of 35% of the water applied (Irrigation + PP) for sugarcane, 29 % for vegetables, 14 % for subtropical trees, 0.45 % for greenhouses, 27 % for unused land and 20 % for urban areas (Figure 29). However, doing the calculations for the hydrological year of 2001, which has a precipitation of 348, close to the mean precipitation of 400 mm, the percentage of water going to deep percolation is lower. The average of the deep percolation from sugarcane fields was 28 %, 22 % for vegetables, 10 % for subtropical trees, 0.27 % for greenhouses, 11 % for unused land and 11 % for urban areas. The amount of deep percolation varies drastically due to variation in precipitation and evapotranspiration, making the percentages inaccurate if used on shorter time periods. The calculated daily deep percolation for the period of October 2001 to September 2012 is therefore used in the model as recharge.

The irrigation rate for sugarcane and subtropical trees is higher during the summer, when evapotranspiration is higher, and precipitation is lower. For vegetables and crops in greenhouses the irrigation rate is highest in February. The excess water percolating to the groundwater is, for most of the crops, lowest during summer, but for sugarcane it is highest in July (Figure 30). During the summer months sugarcane is the only land use that is giving recharge to the aquifer (Figure 30), while in January and February vegetables is the type of land use with highest recharge.

Combining the change in land use from 1956 to 2012 with the calculations of
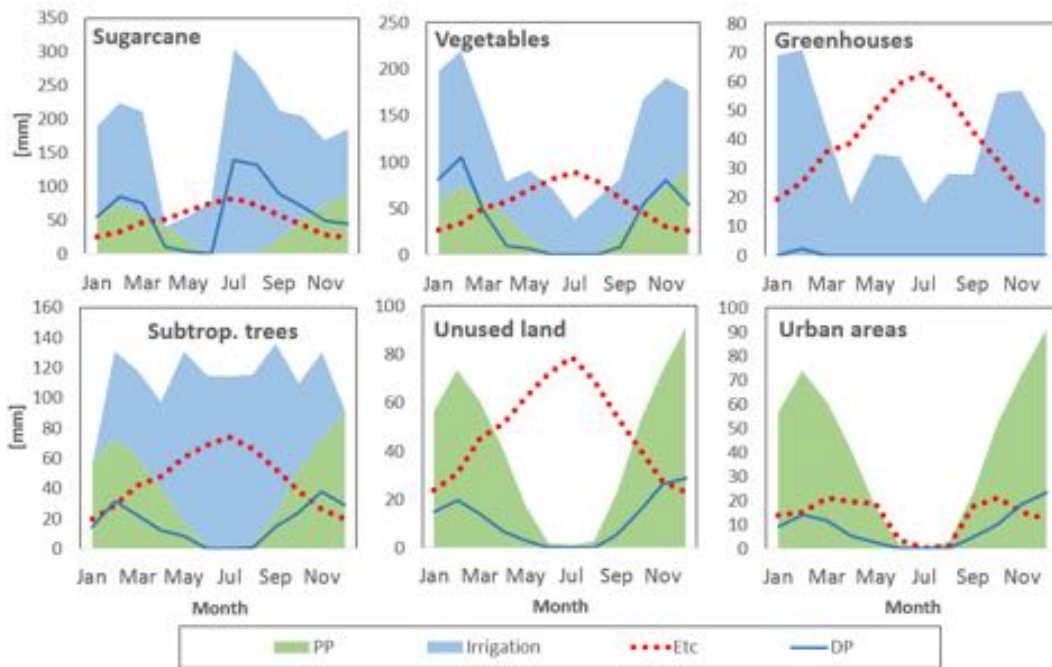
Figure 29: *Monthly average (2001 - 2012) precipitation (PP) and irrigation stacked, together with the calculated monthly deep percolation (DP) and actual crop evapotranspiration (ET_c), for sugarcane, vegetables, greenhouses, subtropical trees, unused land and urban areas.*
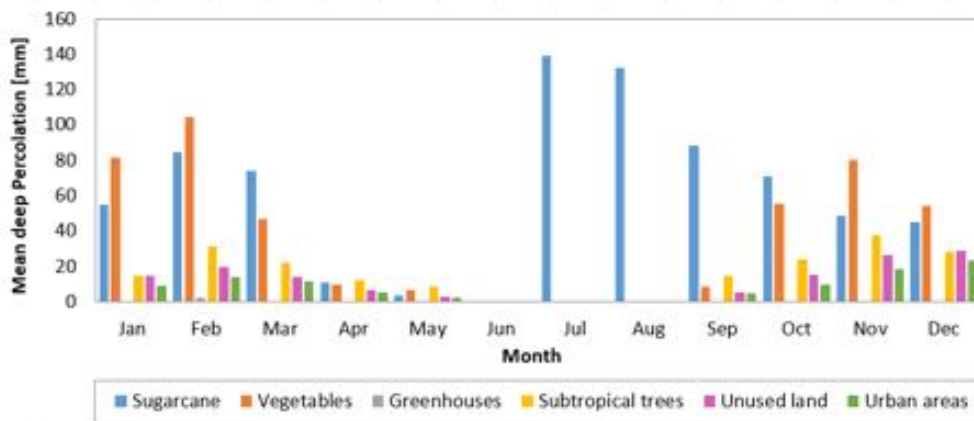
Figure 30: *The average monthly deep percolation for the different land uses (2001-2012).*

recharge for the different categories of land use, the decrease in recharge to the aquifer is calculated. Assuming a precipitation of 400 mm for each year and the percentages of deep percolation for each crop from the year 2001 - 2002, results in a 65 % decrease in annual recharge from 1956 to 2012 (Figure 31A). Looking at the model input with

Figure 31: *The annual recharge calculated with A) the mean precipitation (400 mm), and B) with actual precipitation.*

actual precipitation, the annual recharge is higher, but the decreasing trend is the same (Figure 31B). Both the hydrological year of 2011 and 2012 had precipitation much higher than the average, with 846,7 mm and 724,4 mm respectively, reducing the difference in recharge from previous years.

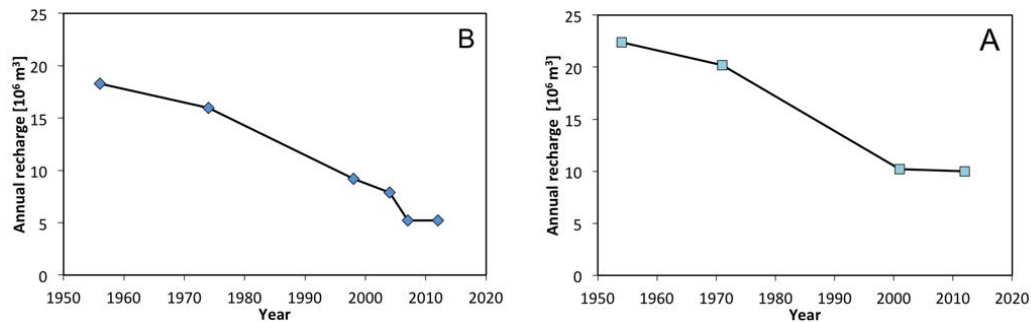## 4.2.1. Comparison of the FAO reference ET and potential ET by Hargreaves and Thornthwaite

The evapotranspiration rate has been calculated with both Hargreaves and Thornthwaite equation in addition to using the FAO Penman-Monteith method to validate the calculated ET_o.

Comparing the calculated Thorntwaite ET_P and the ET_o in a correlation graph (Figure 32) shows that there is some spreading of the values, as the data points are scattered, but there still is a linear trend. The Hargreaves ET_P and the ET_o have a strong correlation and a clear linear trend, but the Hargreaves ET_P data is overestimated with 0.5-1.0 mm d−1 compared to ET_o. Since the Hargreaves equation only contains air temperature and solar radiation, it has a tendency of overestimating the evapotranspiration rates under high relative humidity conditions (Allen et al. 2008; Droogers and Allen 2002). Based on these results, the calculated ET_o used in the recharge calculations seems to be well adjusted to the area.
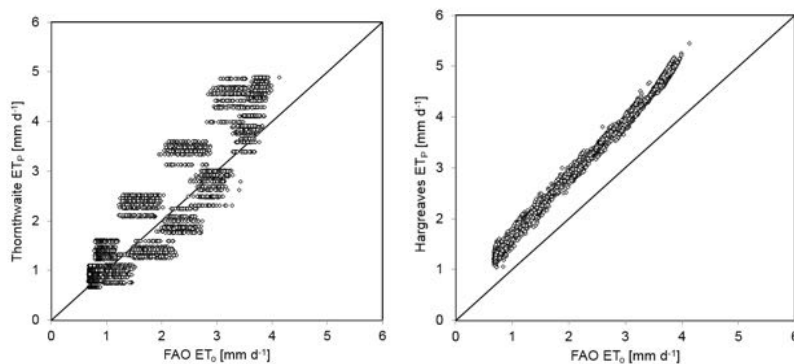
Figure 32: *Relationship between the potential evapotranspiration (ET$_P$), calculated using Thorntwaite and Hargreaves equation (Equation 25 and 26), and the FAO reference evapotranspiration (ET$_o$). The evapotranspiration rates has been calculated using data from October 2001 to September 2012.*

4.3. Hydrogeological model

4.3.1. Aquifer parameters

The main objective of the calibration of this model has been to capture the seasonal fluctuations in the water table and in the hydrological process involved, rather than reaching the lowest absolute error, due to the uncertainties in the hydraulic parameters of the aquifer and the geometry. With both the flow from the Guadalfeo River and the carbonate and the alluvial aquifer in the north affecting the heads in the western area in addition to the recharge on the whole area, this area is the crucial part of the calibration. The calibration process resulted with six different sets of combinations (Table 5), and SET 4 was chosen as the best solution after validation.

Decreasing the conductance of the border of the carbonate aquifer produce too low heads during dry periods. Higher conductance increases the heads in the area, but if too high, it will induce the flow of the groundwater upstream, which is not an hydrogeological optimal solution. Therefore, a high enough conductance to prevent very low heads during dry periods, but without reverting the groundwater flow direction, was selected as the most feasible condition.

Knowing from previous studies (Duque et al. 2009; Calvache et al. 2009) that the river is highly connected to the aquifer, gives reason to assume a high conductance of the river. The conductance of the riverbed was adjusted according to the observed heads in the surrounding wells, making sure it was high enough to give a fast response

47

Table 5: *Calibration of the parameters leading to five sets of combinations.* **C.b. Cond.**: *carbonate border conductance,* **R. HK**.: *river hydraulic conductivity.*

Combination	L.b. Cond.	R. HK	Mean absolute error calibration [m]	Mean absolute error validation [m]
SET 1	0.1	2.2	1.29	2.66
SET 2	0.1	3.0	1.53	2.35
SET 3	0.5	2.2	0.86	2.01
SET 4	**0.5**	**3.0**	**0.85**	**1.70**
SET 5	0.8	1.5	0.82	1.88
SET 6	0.8	2.2	0.86	1.56

Table 6: *Parameters chosen from the calibration and validation process to be used in the numerical groundwater model.*

Parameter	Calibrated value
Carbonate border conductance	0.5
Length of carbonate border	2468 m
Riverbed hydraulic conductivity	3.0 md^{-1}
Riverbed thickness	1 m
Specific yield northern area	0.2
Specific yield south western area	0.3
Specific yield mid area	0.1
Specific yield eastern area	0.2
Hydraulic conductivity	0.4 - 200 md^{-1}

in the groundwater.

Since the hydraulic conductivity and the specific yield is calibrated automatically for the first time period, the model has less error for this period.

Overall, the model shows a good simulation of the natural system in the aquifer, with a mean absolute error of 0.85 m for the calibration period and 1.70 for the validation period (Table 5 and Figure 33). Looking at the two simulated time periods (Figure 34 and 35) shows that the modelled water tables are following the fluctuating trends, even if it misses the highest and lowest peaks.

The model is a simplification of the natural system, and due to the grid size of the model with 100×100 m cells, local differences can produce errors in some of the wells. The largest errors are seen in wells 109 and 63, and comparing the calibration and validation time periods it is clear that the modelled water levels are approximately 1 m lower than observed in the calibration time period, and 2 - 3 m lower in the
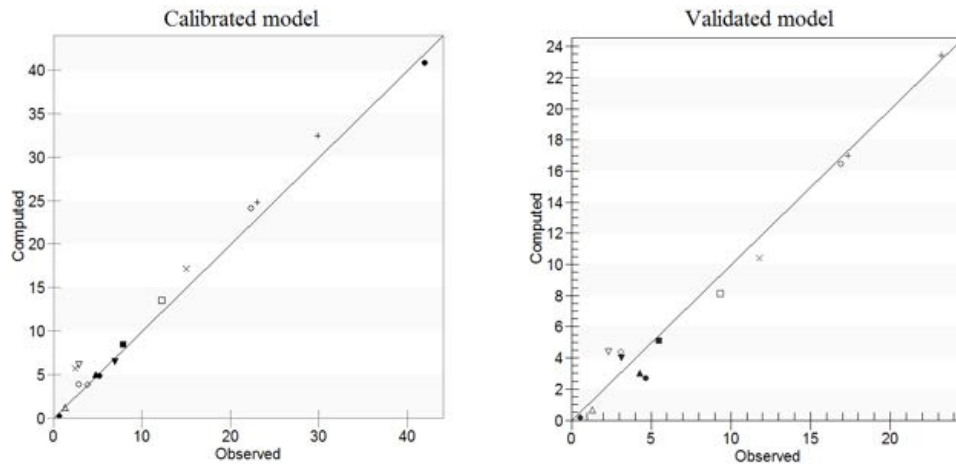
Figure 33: *The computed values of head for the calibrated model (left) and the validated model (right), compared with the observed heads.*

validation period. Well 63 is located approximately 500 m from well 10 (Figure 36) which shows the opposite pattern, with higher water levels in the simulation than in the observed data. The calibration of this area is interpolating the best result between the two to make the error in both minimal, while there probably are some local differences, like small streams or leaking irrigation canals, making the levels different in a small area.

Something similar happens in the area of well 109, as it is surrounded by other wells in addition to being close to the sea the one pilot point in the middle is not able to adjust to the small scale variations in hydraulic conductivity, making consistent error for this well. This area is part of the flood plain of Guadalfeo River where former river channels creates high variability in the characteristics of the soil, which is influencing the water level in each well. As the model is making an average for the cell, it can be assumed that the simulated total flow of the area is not influenced by small local errors.

After the calibration process, the values of mean hydraulic conductivity per cell is ranging from 0.4 to 200 md^{-1} (Figure 37).The north western areas have hydraulic conductivity around 150 - 200 md^{-1}, corresponding to coarse sand and gravel (Dingman 2002), the locations of the old riverbed downstream has a hydraulic conductivity ranging from 50 to 100 md^{-1}, coarse sand, while the former flood plains have the lowest hydraulic conductivity, ranging from 0.4 to 30 md^{-1}, loam to medium sand. The

Figure 34: *The calibration of the model was done using data from October 2001 to September 2007. Calculated heads illustrated with the black line, and observed heads as the midpoint of the error bars. The error bar is showing the observed head ± 1 m. Green and yellow colour of the error bars symbolises error less than 1 m, while red colour symbolises more than 1 m error.*
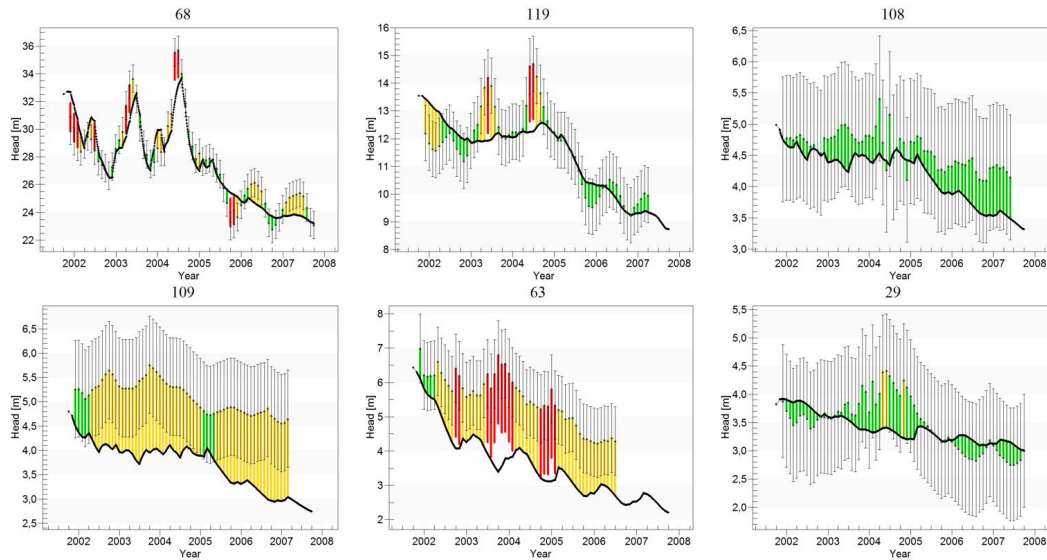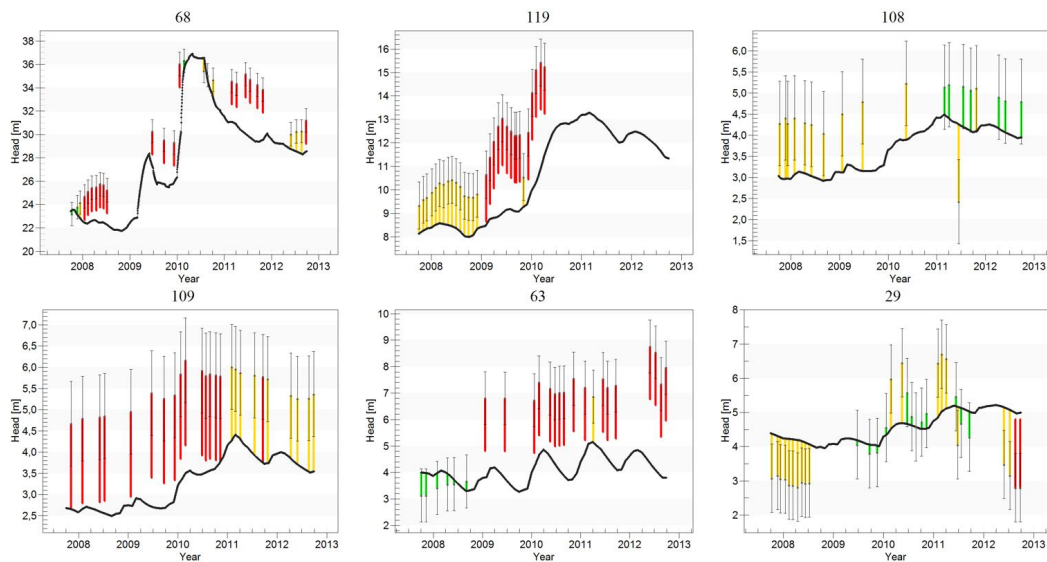

Figure 35: *The validation of the model was done using data from October 2007 to September 2012. Calculated heads illustrated with the black line, and observed heads as the midpoint of the error bars. The error bar is showing the observed head ± 1 m. Green and yellow colour of the error bars symbolises error less than 1 m, while red colour symbolises more than 1 m error.*
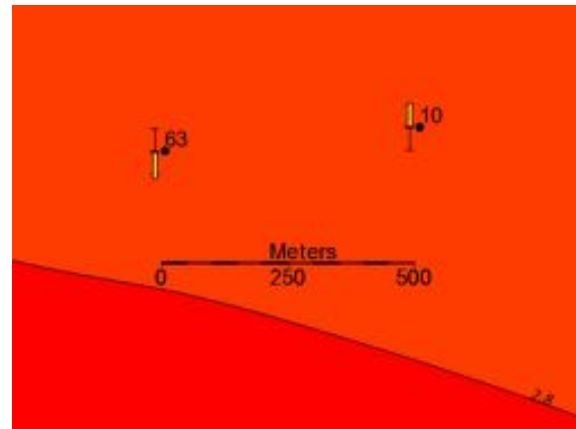
Figure 36: *Well 63 and 10 are located only 500 m apart, but have approximately 2 m difference in water level.*
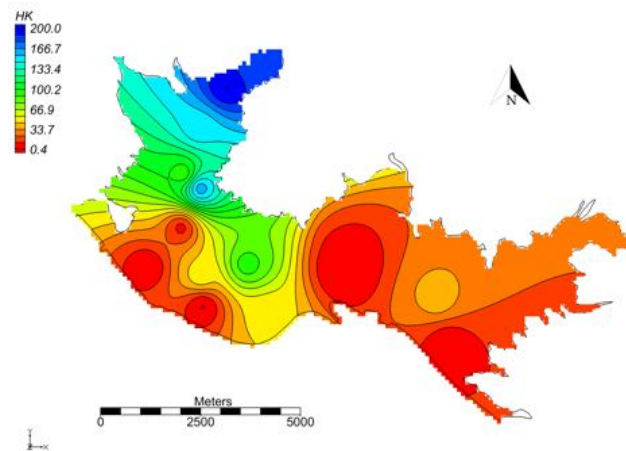
Figure 37: *The modelled mean hydraulic conductivity of each cell in the aquifer, ranging from 0.4 to 200 md^{-1}*

areas far from the river and other inflows are more consistent at around 25 md^{-1}, which corresponds to medium sand.

The specific yield was calibrated to be ranging from 0.1 to 0.338 (Figure **??**). In the northern area with highest hydraulic conductivity, the specific yield was calibrated to be 0.2 (or 20 %), corresponding to gravel (Freeze and Cherry 1979). The south western area had a specific yield of 0.3, coarse sand, while the eastern floodplain area was calibrated to have a specific yield of 0.1, silt to fine sand. The specific yield in the eastern area was 0.2, which in addition to correspond to gravel, also is the value of fine to medium sand.
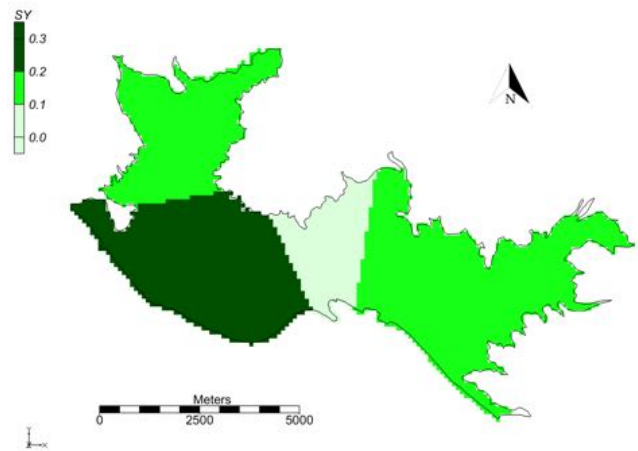
Figure 38: *The modelled specific yield of the aquifer, ranging from 0.2 to 0.36*

4.3.2. Flow budget

The flow budget of the aquifer is varies depending on the natural variations in incoming river flow and precipitation (Figure 39), connected to the seasonal changes with dry summers and rain concentrated in the fall and spring.
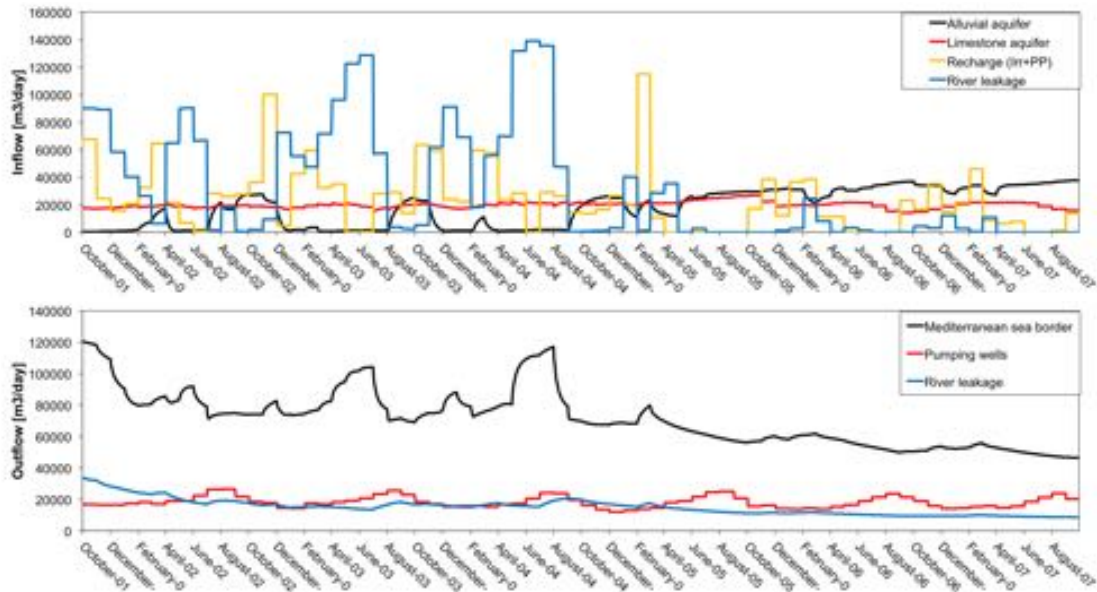
Figure 39: *The flobudget for the aquifer from October 2001 to September 2007.*

In the calibrated model from October 2001 to September 2007, most of the inputs are coming from river leakage and surface recharge (from irrigation and precipitation).

The maximum recharge proceeding from the river is up to 140 000 m³/day during the period with highest precipitation. During summer, the flow in the river is low, and the main input to the aquifer is the recharge, mainly from irrigation. The flow from the alluvial aquifer is lower with around 500 - 1000 m³/day when the flow in the river is high, but it increases to up to 35 000 m³/day when there is little or no flow in the river. This is also evident as seasonal trends, with higher flow rates from the alluvial during the summer periods. The flow from the carbonate aquifer is relatively stable throughout the whole time period at 20 000 m³/day. This might be because the water table used for the carbonate aquifer has been too high, as the actual water table along this border is not known. If the water table in the carbonate aquifer has a higher altitude than the water table in the detrital aquifer at all time, it will be continuous inflow according to the conductance. Since the levels in the well representing the carbonate aquifer follows the same trends as the other wells (Figure 8), the flow will be constant as long as the heads along the border is not alternating differently.

Most of the flow from the aquifer is discharging to the sea along the coastline, while the pumping outputs and the flow gained by the Guadalfeo River, where the water table exceeds the level of the riverbed, are inferior. The amount of discharge to the river is ranging from 20 000 m³ during the wet period, to less than 10 000 m³/day during the dry periods, evident as a decreasing trend throughout the calibration time period. The outgoing flow is directly connected with the incoming flow, with almost immediate reactions showing that the aquifer has a fast response time.

In the period from 2008 to 2012 (the validation time frame), the same patterns can be seen as in the period from 2001 to 2007, with incoming flow from the alluvial aquifer of up to 20 000 m³/day in the dry period from 2008 to 2009 (Figure 40). In 2010 the precipitation was much higher than average, causing the incoming flow from the river to increase to as much as 370 000 m³/day. While most of the water is flowing out through the border along the coast, the large increase in inflow in 2010 is followed by an increase of discharge to the river downstream from approximately 12 000 m³/day to almost 50 000 m³/day. Even with these large changes of river flow, the flow from the carbonate aquifer is relatively stable at 25 000 to 30 000 m³/day of flow, except an abrupt decrease for a short period of time simultaneously with the
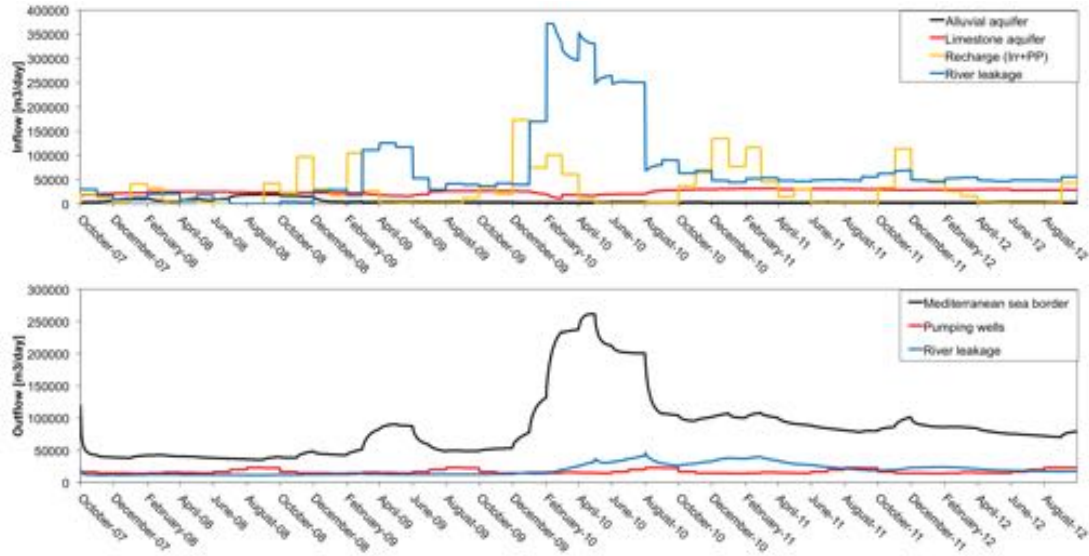
Figure 40: *The flowbudget for the aquifer from October 2007 to September 2012.*

highest amount of flow in the river.

4.4. Historical scenarios

In the simulation of the 1950's most of the inflow to the aquifer is coming from recharge from irrigation (Figure 41), with the largest amounts in July with 140000 m^3/day. The river is contributing from November to June, with the highest incoming flow rates at almost 130000 m^3/day during the wet years, 1956 and 1960, while the highest flow during a normal year is less than 90000 m^3/day. The incoming flow from the alluvial aquifer in the north is highest in late summer and autumn, when the river flow is low. The highest flow rate is approximately 20000 m^3/day. The flow from the carbonate aquifer is relatively stable at around 20000 m^3/day.

The discharge to the Mediterranean Sea in the 1950's fluctuates from 70000 m^3/day to 170000 m^3/day at the largest. In 1956 and 1960, which had the highest river flow, and the highest discharge to the sea. The outgoing flow to the river is fluctuating around 20000 m^3/day with increased flow from July to January, corresponding with the highest recharge rates from irrigation and precipitation. The pumping rates is in the 50's is 26000 m^3/day.

In the 1970's the recharge from precipitation and irrigation is still the main con-

54
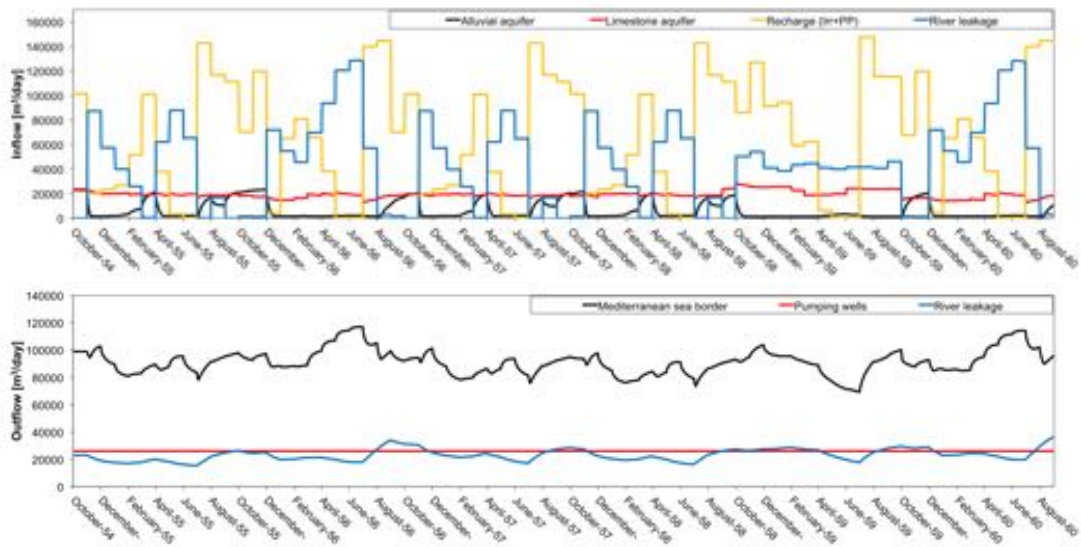
Figure 41: *The flowbudget of the aquifer for the simulation of the 1950's.*

tributor to the total inflow, with peak recharge in July or August, varying from 120000 m^3/day to 145000 m^3/day (Figure 42). The river outflow into the aquifer has peaks in November or December and May or June, with the normal peak flow being around 80000 m^3/day, a decrease of almost 10000 m^3/day from the 50's. The inflow from the alluvial aquifer is reaching 35000 m^3/day in the 70's during the normal peak periods, and as much as 40000 m^3/day when there is no flow from the river (1975). The carbonate aquifer is contributing with an inflow of approximately 25000 m^3/day.

The biggest change between the simulation of the 50's and the 70's is the increased withdrawals of groundwater for industrial use. The total pumping rate for the whole aquifer in the 70's is 41000 m^3/day, an increase of 15 m^3/day from the 50's. While the discharge to the Mediterranean Sea stays fluctuating at around 90000 m^3/day, the increased pumping causes the discharge to the river to decrease to 11000 m^3/day.

4.4.1. Hydrodynamical changes

Comparing the recent years with the simulated periods there are some clear differences in both flow patterns and water levels. In the 1950's, the water level is even from west to east (Figure 43), because of the distribution of river water for irrigation of the sugarcanes. The 1970's (Figure 45b) had low heads due to high pumping rates,

55
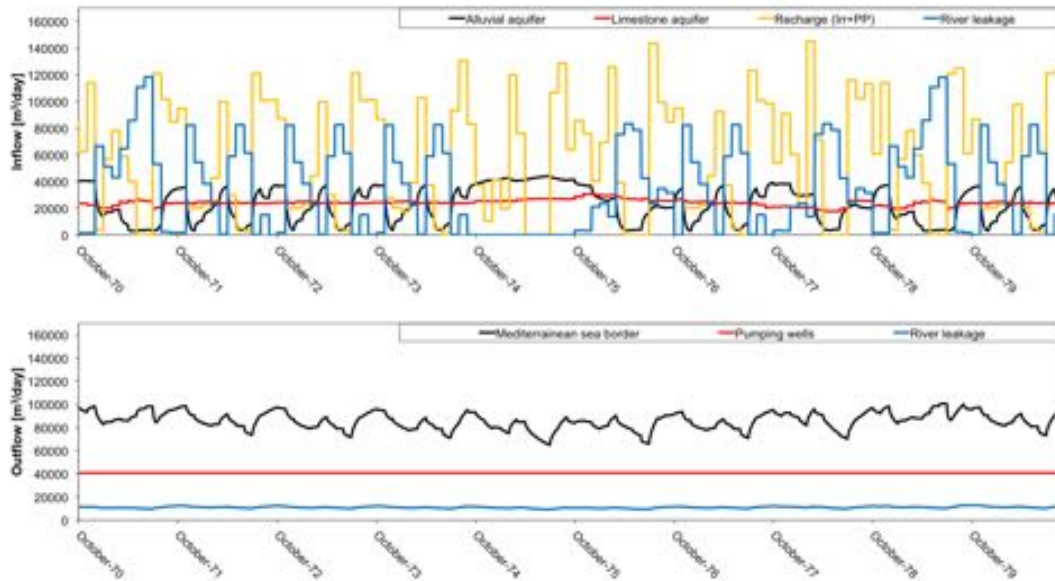
Figure 42: *The flowbudget of the aquifer for the simulation of the 1970's.*

making the change from the 70's to recent years very little (Figure 45e). However, looking at the changes from 1959 to 2012, the levels are clearly declining (Figure 45f). The difference in heads are increasing at distance from the coastline, and the differences in water levels from 1956 to 2012 are very large at higher elevations in the eastern sector (Figure 46). The dataset for 2012, used for calculating the difference in heads is at the end of the hydrological year, after having two very wet years with precipitation above average. This indicates that the changes seen between the model of 2012 at the simulated 50's, are at this time low due to elevated levels, meaning that the 2 m changes in vicinity of the river is a minimum of what could be observed during periods with mean precipitation.

The interactions between the Guadalfeo River and the aquifer is not only affecting the water budget, but also the groundwater flow-direction. The Guadalfeo River is loosing water to the aquifer along most of its course, but close to the river mouth, the river is gaining water at all times (Figure 45a to 45d). But in the 1950's the river is also gaining water at higher elevation (Figure 46), acting as a drain for almost half of its track over the aquifer. Currently it has a very minor gaining character, being mainly an effluent river. This process has been observed by differential gauging
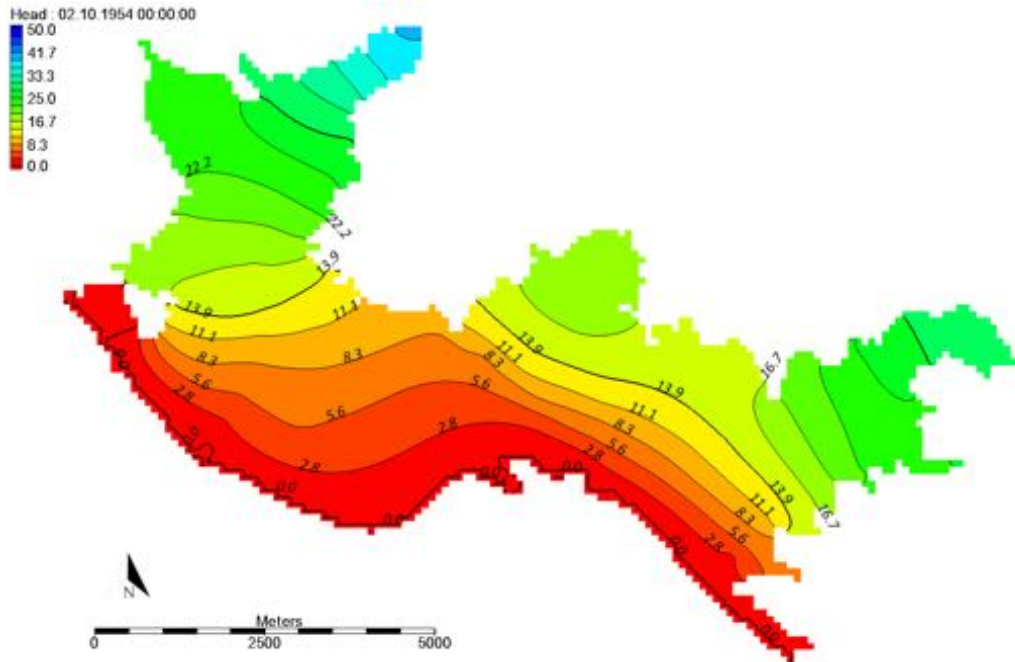
Figure 43: *The water level in the simulation of the 1950's.*

during punctual field surveys.
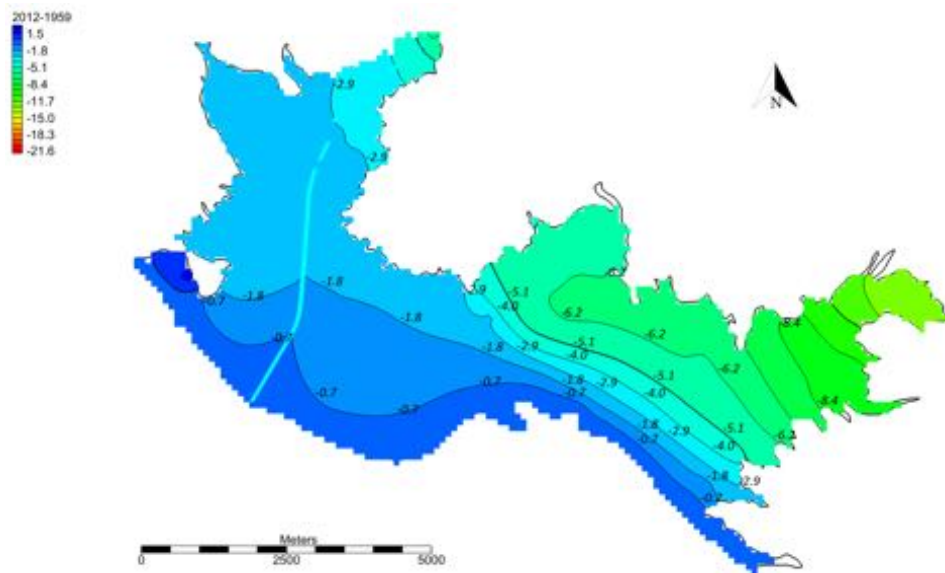
Figure 44: *The change in levels from the simulation of 1956 to the model of 2012.*

(a) *1950's*

(b) *1970's*

(c) *01-11-2001*

(d) *30-09-2012*

(e) *2009-1978*

(f) *2012-1959*
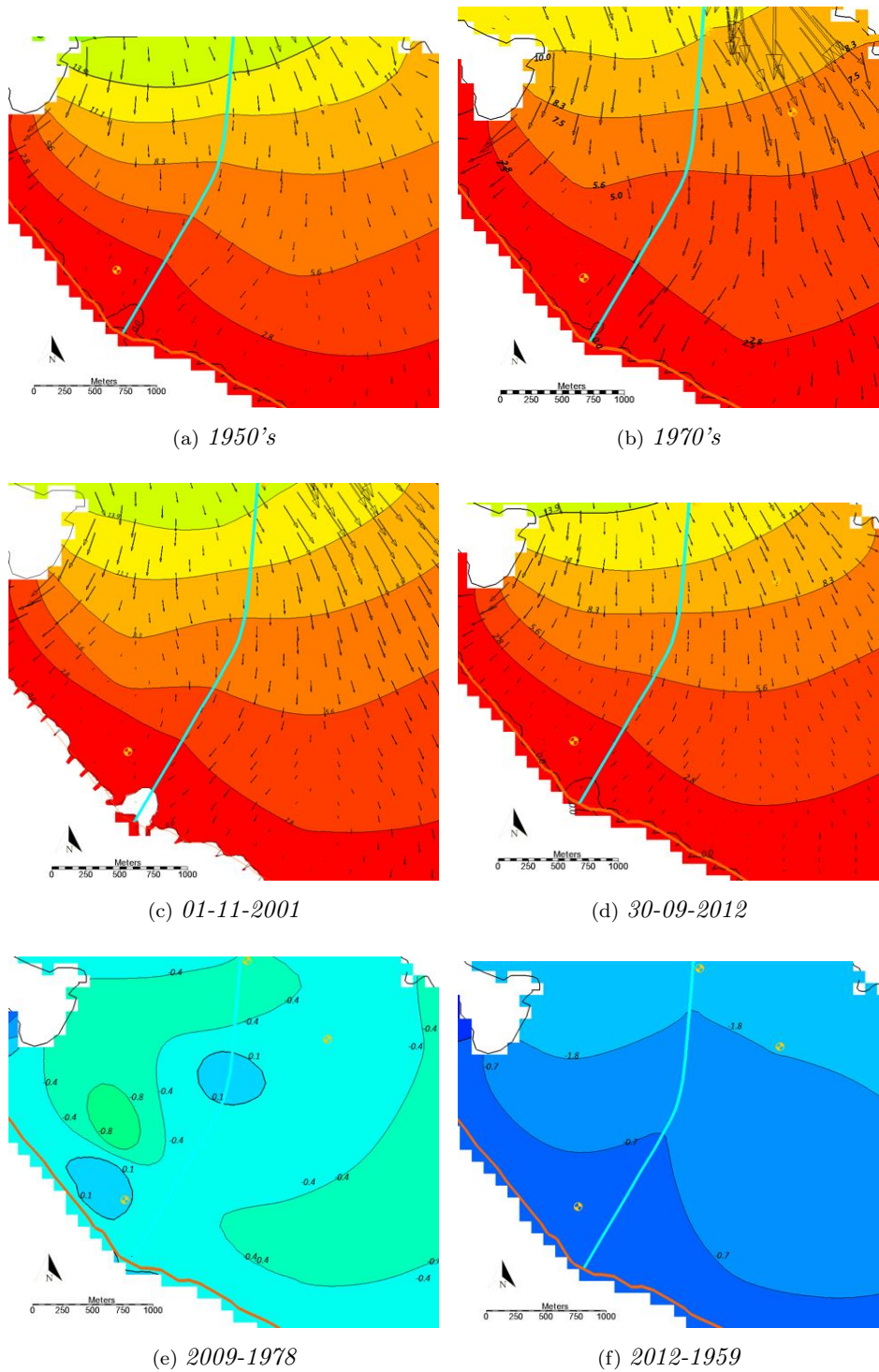
Figure 45: *The flow pattern and water levels in the area adjacent to the river mouth in the simulated time periods, 1950's and 1970's, and in model in 2001 and 2012. 45e and 45f shows the difference in water levels between 2009 and 1978, and 2012 and 1959, respectively.*
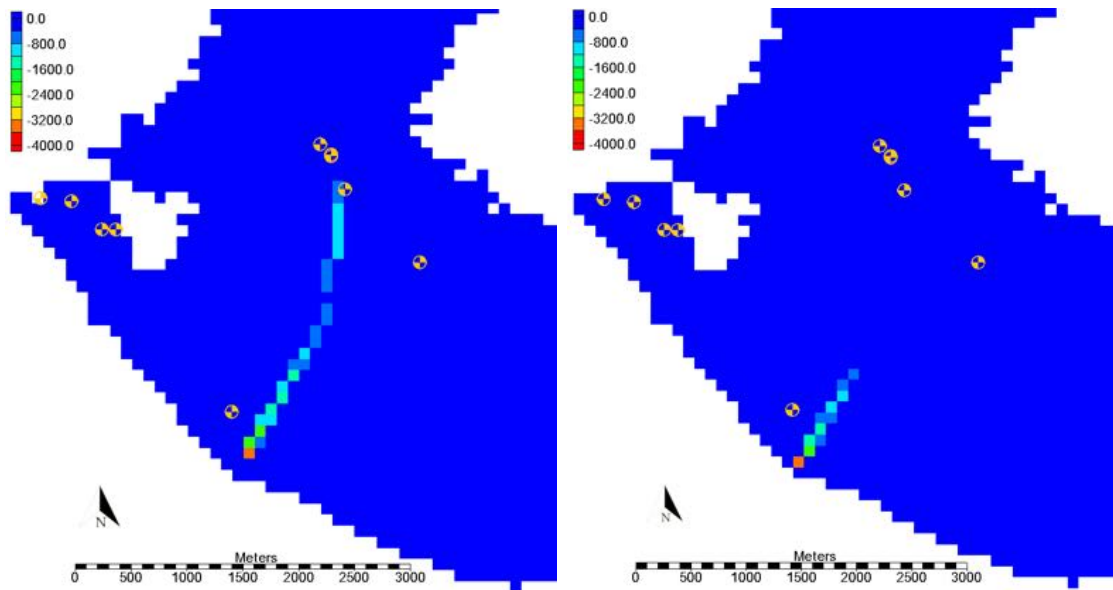
Figure 46: *The leakage from the aquifer [m^3/day] into the river for 1959 (left) and 2012 (right).*

5. DISCUSSION

5.1. Land use changes and change in recharge

The land use maps from the satellite images from the last 60 years shows clear change in land use, with the abrupt disappearance of the sugarcane crops, and the increase in other agricultural crops. From a recharge perspective, this has a big impact, as the calculations previously presented that sugarcane is the crop with the highest recharge rate.

5.1.1. Recharge of the aquifer from deep percolation

The estimated recharge resulting from the deep percolation computations indicate that the recharge is a large part of the total inflow to the aquifer, and changing it may result in large long term effects. However, the other sources of inflow increase their flow when the recharge decreases. This is because the boundary conditions are head dependent, making the inflow larger when the difference increases. This causes the changes in heads due to a decrease in recharge being minor on a small time scale, as the levels are fluctuating due to wet and dry years. Droughts or wet periods are both defined as shorter periods of precipitation below or over the normal or mean precipitation, which will be followed with other periods that brings the aquifer back to average state. In contrary to temporary climate conditions, the change of land use may in a long term perspective result in significant, and maybe even permanent, effects to the aquifer.

The amount of water percolating during irrigation and/or rainfall has been established following a method by the Food and Agriculture Organization of the United Nations, which is based on the Penman-Monteith equation. Other methods that consider more local factors, as looking at water table fluctuation or measuring the soil moisture at different depths underneath the different crops, was not available for this study. The aquifer is too intricate for the water-table fluctuation (WTF) method (Healy and Cook 2002), since removing one of the inflows only increases the flow in one of the other, and that the changes are too long-term based to be reflected in the water table without disturbance by natural fluctuations. Using measurements

of the soil moisture requires installed equipment under each land use, which was not available in the field of study. Different studies using different methods, some field measuring and some only modelling or calculating, shows that there is a range of different percentages of irrigated water deep percolating, dependent on the local factors.

The irrigation by flooding of furrowed fields have the most varying values of deep percolation. The type of soil and how the furrows are placed are affecting how much of the water is running off on the surface, and how much that is infiltrating. Field measurements by the USGS (Arnold 2011) using an unsaturated zone water-balance (UZWB) method, showed approximately 29 % of percolation of precipitation plus irrigation for their first year of measurements, and 39 % percolation for the second year when the precipitation was higher. Using the water-table fluctuation (WTF) method on the same field the percolation was 32 % for the first year. Another study estimated the deep percolation when flooding sugarcane fields to be ranging from 8 % (medium clay) to 26 % (sillty clay loam) (Thorburn et al. 2011). Previous studies of the Motril-Salobreñ aquifer have assumed 30 % deep percolation when irrigating sugarcane, 20 % for subtropical trees, 5 % for greenhouses and 25 % for vegetables (IGME 1999; Calvache et al. 2009). The estimation of deep percolation using the FAO Penman-Monteith method provided similar values to the percentages in the previous studies, with 28 % deep percolation for sugarcane in 2001, when the precipitation was close to the mean precipitation. Comparing the deep percolation calculated with a previous study on cherimoya and mango trees in the same area (Pleguezuelo et al. 2011) shows a similar trend, with more deep percolation in the autumn than in the spring, with measured deep percolation ranging from 2 to 14 mm monthly. For comparison, the calculations in this study resulted in a monthly average of deep percolation from 2001 to 2012 of 16 mm. The previous field study (Pleguezuelo et al. 2011) is not presenting the amount of irrigation used, making it difficult to compare the amount of deep percolation. From the comparison with previous studies it is reasonable to rely on the results of the performed calculations.

5.1.2. *Water balance*

The recharge of the aquifer from deep percolation is a significant part of the total recharge accounting for 25 % of the total inflow in 2012. However, in 1956 the surface recharge was contributing with as much as 48 % (Table 7). As the percentage of crops that needs less water is increasing, the vertical recharge to the aquifer is decreasing. The amount and significance of this is however not homogeneous for the different areas. Compared to precipitation and recharge from the river, the irrigation might not have the biggest impact on the groundwater close to the river channel. Further from the river channel the recharge from precipitation and irrigation is the most important factor to maintain the current water table head.

The water budget of the aquifer has previously been estimated by several other studies (Castillo 1975; CHSE-YRIDA 1984; ITGE 1988; Heredia et al. 2003; Ibáñez 2005) (Table 7). The most uncertain factor in this groundwater balance is the incoming flow from the carbonate aquifer in the north, as the length of the stretch where the detrital sediments are in contact with the carbonates (as seen in Figure 19) and the decrease of the water table along the border are unknown. The previous studies has estimated a low contribution of flow from the carbonate aquifer, with around 4 Mm^3/year. With a longer time period for calibration and validation, this study suggests that the water levels in the aquifer may be more depending on the flow from the carbonate aquifer than previously estimated, with flowrates ranging from 6.8 to 10.6 Mm^3/year. During calibration, lower conductances of this border resulted in heads much lower than observed during periods with low river flow. While the flow from the carbonates was higher, the flow from the alluvial sediments surrounding the river was lower than in previous studies, and especially low during the wet years, reaching a minimum flow of 1.1 Mm^3/year. The flow into the aquifer from the alluvial aquifer is larger when the recharge from other sources is smaller, like the river flow and surface recharge. This indicates that the the river is always loosing water to the alluvial, even when the flow is low. When the flow in the river and the surface recharge is large, the flow from the alluvial gets blocked by high water levels in the north.

The volume of inputs and output varies between different years due to the climatic environment with varying precipitation and inflows, in addition to anthropogenic

activity which is altering the aquifer surface. The hydrological year of 2012 had a precipitation of 724 mm, making the total input be larger than in 2001. However, even with an increase of precipitation from 348 mm, the surface recharge still had a minor decrease from 10.2 to 10.0 Mm^3/year, caused by the decrease in irrigation (Figure 28).

Since the previous studies are performed at different years, it is interesting to look at the differences in recharge for the different years, and compare them with the simulated years. The two earliest studies (Castillo 1975; CHSE-YRIDA 1984) might have underestimated the recharge from irrigation and precipitation, but the last three studies (ITGE 1988; Heredia et al. 2003; Ibáñez 2005) have assumed recharge which correlates with the period between the 70's and 2001 in the simulations in this study.

Table 7: *Estimated water budget of the Motril-Salobreña aquifer for the modelled years 2001 and 2012, and the two scenarios of the 1950's and 70's, and by previous studies for comparison. * Precipitation + Irrigation.*

Inputs and Outputs [$Mm^3/year$]	1950's	1970's	2001	2012	Castillo (1975)	CHSE (1974)	ITGE (1988)	Heredia (2003)	Ibáñez (2005)
North alluvial	3.2	7.5	2.6	1.1	13	25	15.5	3.5	4.7
Carbonate aquifer	7.2	8.8	6.8	10.6	6	3	2	4	4.2
River infiltration	13.5	12.7	16.9	19.1	47	13	11.5	11.6	11.5
Recharge*	22.4	20.2	10.2	10.0	14-19	9	16.9	16.8	13.6
Others	-	-	-	-	15-20	3	1.4	-	-
Total input	46.3	49.2	36.5	40.8	60-70	53	47.3	35.9	34
Pumping	9.4	14.9	7.2	6.2	-	25	17.1	15.4	7.5
Aquifer to the river	7.1	4.2	8.4	7.4	-	-	-	0.4	0.3
Discharge to the sea	33	31.9	32	30	40-45	22	30.2	16.8	26.2
Others	-	-	-	-	6-10	6	-	1.8	-
Total output	49.5	50.9	47.6	43.5	62-71	53	47.3	34.4	34

* Precipitation + Irrigation

With eight wells placed along the river, and the same amount of pilot points, the hydraulic conductivity along the river course is assumed to be well calibrated. The average values of hydraulic conductivity from calibration correspond to the materials found in the boreholes, which supports this. However, in the southern part of the aquifer the characteristics are assumed to be more heterogeneous than further north (see Section 2.2), which may be the cause of some of the errors seen during the calibration and validation process. The distribution of hydraulic conductivity

is previously shown to have a great affect on river-aquifer interaction (Fleckenstein et al. 2006). The river-aquifer interactions close to the sea may therefore have some limitations, due to the cell size in the model, which is unable to capture small-scale heterogeneity in the hydraulic conductivity. Also, the presence of some small streams not considered in the model, might affect nearby wells with lowering or decreasing the heads.

5.2. Scenarios of the past and a perspective on the future

The simulation of the 1950's considers excess water from flooding of sugarcane fields as the main surface recharge, in addition to precipitation. This have been the state of the aquifer for centuries, keeping the water level in the whole aquifer close to the surface. With a high irrigation rate distributed over the whole aquifer, the water level is at the approximate same elevation at different distances from the river (Figure 43).

The simulation of the 1970's combined the effects of increased groundwater withdrawal, irrigation reduction and natural climate variations. The increased pumping rates, with almost 5 Mm^3/year, made the discharge to the river decrease drastically, and lowered the water table underneath the riverbed elevation. In comparison, the decrease in recharge was only 2.2 Mm^3/year, making it difficult to detect changes to land use change not related to the increased pumping rates.

The decrease of water withdrawals since the 1970's may have prevented a possible change in water levels due to the changes in land use. As the pumping rates have decreased from 15 Mm^3/year in 1975 and a staggering 28 Mm^3/year in the 80's (Figure 11) to 6.2 Mm^3/year in 2012, the surface recharge has decreased with 12.4 Mm^3/year during the period from 1954 to 2012. The decrease in recharge is less than the decrease in water withdrawals considering the pumping in the 80's, which may explain why there is no detectable declining trend in water levels in the wells for this period (Figure 8d). Only looking at the change from the 50's to the last years, the decrease in pumping is less than the decrease in recharge, making it possible to assess the effects from land use change. The water level have clearly decreased since the aquifer covered mainly by sugarcane, and the recharge calculations indicate that the levels will continue to decrease if the amount of greenhouses increases.

6. CONCLUSIONS

Six land use maps were constructed to map the distribution of the different land uses, and how it has been changing during the last 60 years. Based on analysis of satellite images of different years, the areas corresponding to each type of crop have been calculated. In 1956 the land use was distributed as 70 % sugarcane, 22 % unused land, 4 % urban areas and 3 % subtropical trees of at total area of 42 km^2. By 2012 sugarcane have been reduced by 100 %, while subtropical trees have increased to cover 32 %, and greenhouses, vegetables and urban areas have increased to a 32 %, 21% and 20 % coverage respectively. Unused land have been reduced to cover 13 % of the aquifer area in 2012.

The shift in agriculture have resulted in a reduction of water used for irrigation of 28 Mm^3/year, from 1956 to 2012. The amount of recharge produced by the different land uses are greatly dependent on the amount of precipitation. For 2001, which had precipitation close to the mean for the area, the recharge by sugarcane fields was 28 % of the total amount of precipitation and irrigation, by vegetables it was 22 %, 10 % for subtropical trees, 0.27 % for greenhouses, 11 % for unused land and 11 % for urban areas. The decrease of irrigation due to land use change have caused an estimated 65 % reduction in surface recharge.

A numerical flow model of the Motril-Salobreña aquifer was calibrated for the period from 2001 to 2007 and validated from 2007 to 2012, with a mean absolute error of 0.85 m for the calibration period and 1.70 for the validation period. The hydraulic conductivity of the aquifer was calibrated using the pilot points technique to range from a maximum of 200 md^{-1} in the northern sector to a minimum of 0.4 md^{-1} in the areas close to the coastline. The specific yield was estimated in zones, delimited by the distribution of hydraulic conductivity and calibrated with PEST, ranging from 0.1 to 0.3. The conductance of the riverbed was estimated as 3 md^{-1}, while the conductance of the boundary between the carbonate aquifer and the Motril-Salobreña was estimated as 0.5 md^{-1}.

From 2001 to 2012 the water levels in the aquifer are fluctuating with up to ± 5 m in the northern sector due to natural annual variations in climate. The fluctuations are reduced closer to the sea and at distance from the Guadalfeo River,

with fluctuations less than 2 m in the southern areas. However, a prolonged reduction in irrigation would according to the simulations be larger than that of a brief drought, causing long term, and maybe even permanent effects to the aquifer.

Two scenarios of the past have been simulated to study the condition under previous land use distribution, the 1950's and the 1970's. The application of the numerical groundwater model coupled with the recharge estimates allows the assessment of how the reduced irrigation is influencing the hydrodynamics. From 1956 to 2012 the water levels have been reduced by 1 - 2 meters in the lowlands and in vicinity of the river, while the eastern area have had a simulated decrease of up to 10 m. The larger decrease in the east is a result from that the irrigation of sugarcane distributed water from the Guadalfeo River to areas that otherwise were not influenced by river leakage, artificially increasing the heads to an even level from west to east.

The change in water levels affect the flow in the aquifer surrounding the river. Areas where the aquifer previously discharged into the river, are now having little or no interaction. In the 1950's, the last 3 km of the river stretch (of a total of 7 km crossing the aquifer) was gaining water from the aquifer. In 2012 the stretch that is gaining water has decreased to approximately 1000 m. This is a significant change in the hydrodynamics of the aquifer.

REFERENCES

Abou Lila, TarekSelim, Ronny Berndtsson, Magnus Persson, Mohamed Somaida, Mohamed El-Kiki, Yasser Hamed, and Ahmed Mirdan (2013). "Numerical evaluation of subsurface trickle irrigation with brackish water". In: *Irrigation Science* 31.5, pp. 1125–1137.

Alexandratos, Nikos and Jelle Bruinsma (2012). *World Agriculture Towards 2030/2050: the 2012 revision.* ESA Working Paper 12-03. Food and Agriculture Organization of the United Nations - Agricultural Development Economics Div.

Ali, M. H. (2010). *Fundamentals of Irrigation and On-farm Water Management: Volume 1.* Springer-Verlag New York, p. 560.

Allen, Richard G., Luis S. Pereira, Dirk Raes, and Martin Smith (2008). "Crop Evapotranspiration". In: *FAO Irrigation and Drainage Paper* No. 56.

Alonso-Martinez, J., J. Arjona Garcia Borreguero, A. Ballester Rodriguez, F.J. Elorza Tenreiro, M. Gómez Sánchez, R. Hernández Manchado, M. Hervás Maldonado, A. Iglesias López, T.E. Iglesias Delgado, J. López Bravo, J.A. López Geta, A. de Mera Merino, and J.I. Ortiz López (2000). *Hidrobas v 3.0 win.* Available at: http://aguas.igme.es/igme/aplicaciones/Hidrobas.htm. Instituto Geológico y Minero de España y Universidad Politécnica de Madrid.

Aquaveo, L.L.C. (2015). "Groundwater Modeling System Version 10.0". In: *UT, USA*.

Arnold, L.R. (2011). "Estimates of Deep-Percolation Return Flow Beneath a Flood- and a Sprinkler-Irrigated Site in Weld County, Colorado, 2008-2009". In: *USGS: Scientific Investiagtion Report 2011-5001.*

Austin, Nick R., J. Bernard Prendergast, and Matthew D. Collins (1996). "Phosphorus Losses in Irrigation Runoff from Fertilized Pasture". In: *Journal of Environmental Quality* 25 (1), pp. 63–68.

Ayars, J. E., C.J. Phene, R.B. Hutmacher, K.R. Davis, R.A. Schoneman, S.S. Vail, and R.M. Mead (1999). "Subsurface drip irrigation of row crops: a review of 15 years of research at the Water Management Research Laboratory". In: *Agricultural Water Management* 42.1, pp. 1–27.

Ayuntamiento de Motril (2015). *Motril Turismo (Tourist Information of Motril).* URL: http://motrilturismo.com/en/.

REFERENCES

Barnes Jr., H.H (1967). *Roughness characteristics of natural channels.* Water-Supply paper 1849. U.S. Geological Survey. Washington, U.S.A.

Benavente, J. (1982). *Contribución al concocimiento hidrogeológico de los acuíferos costeros de la Provincia de Granada.* Ph.D. University of Granada, Spain.

Benavente, J. (1985). *Las aguas subterráneas de la Costa del Sol de Granada.* University of Granada County Council. Granada, Spain.

Bethune, M. G., B. Selle, and Q. J. Wang (2008). "Understanding and predicting deep percolation under surface irrigation". In: *Water Resources Research* 44.12.

Calvache, M. L., S. Ibanez, C. Duque, W. Martin-Rosales, M. Lopez-Chicano, J. C Rubio, A. Gonzales, and C. Viseras (2009). "Numerical modelling of the potential effects of a dam on a coastal aquifer in S. Spain". In: *Hydrological Processes.*

Calvache, M.L., C. Duque, F. García-García, J.M. Soria, M. López-Chicano, and C. Viseras (2010). "Towards the stratigraphic anatomy of the Motril-Salobreña coastal aquifer. Information from well cuttings and logs". In: *18th International Sedimentological Congress.* Mendoza, Argentina.

Castillo, E. (1975). *Hidrogeología de la Vega de Motril-Salobreña y sus bordes.* PhD thesis. University of Granada, Spain.

Christopherson, Robert W. (2009). *Geosystems, An Introduction to Physical Geography.* Seventh edition. New Jersey, USA: Pearson Education, Inc.

CHSE-YRIDA (1984). "Estudio de viabilidad de la ampliación de la zona regable de Motril-Salobreña hasta la cota 300." In:

Dahlhaus, Peter G., Timothy J. Evans, Erica L. Nathan, Jim W. Cox, and Craig T. Simmons (2010). "Groundwater-level response to land-use change and the implications for salinity management in the West Moorabool River catchment, Victoria, Australia". In: *Hydrogeology Journal.*

Delin, Geoffrey N., Richard W. Healy, Matthew K. Landon, and John Karl Böhlke (2000). "Effects of topography and soil properties on recharge at two sites in an agricultural field". In: *Journal of the American Water Resources Association* 36.6, pp. 1401–1416.

Dingman, S. Lawrence (2002). *Physical Hydrology.* second edition. Waveland Press, Inc.

Doherty, J. (1998). *PEST: Model Independent Parameter Estimation.* 5th edition.

Doherty, John (2003). "Ground Water Model Calibration Using Pilot Points and Regularization". In: *Ground Water* 41 (2), pp. 170–177.

Droogers, P. and R. G. Allen (2002). "Estimating refernce evapotranspiration under inaccurate data conditions". In: *Irrigation Drainage Systems* 16.-, pp. 33–45.

Duque, C., M. L. Calvache, and P. Engesgaard (2009). "Investigating river-aquifer relations using water temperature in an anthropized environment (Motril Salobreña aquifer)". In: *Journal of Hydrology*.

Duque, C., M. L. Calvache, A. Pedrera, W. Martin-Rosales, and M. Lopez-Chicano (2007). "Combined time domain electromagnetic soundings and gravimetry to determine marine intrusion in a detrital coastal aquifer (Southern Spain)". In: *Journal of Hydrology*.

Duque, C., M.L. Calvache, A. Pedrera, A. Hodar, M. Lopez Chicano, W. Martin Rosales, A. Gonzales, and J.C. Rubio (2006). "Characteristics of the fresh water-salt water contact in the Motril-Salobreña aquifer (Southern Spain) using time domain electromagnetic soundings". In: *Proceedings 1st SWIM-SWICA Joint Saltwater Intrusion Conference*.

Duque, C., M. López-Chicano, M. L. Calvache, W. Martín-Rosales, J. M. Gómez-Fontalva, and F. Crespo (2011). "Recharge sources and hydrogeological effects of irrigation and an influent river identified by stable isotopes in the Motril-Salobreña aquifer (Southern Spain)". In: *Hydrological Processes* 25.14, pp. 2261–2274. ISSN: 1099-1085. DOI: 10.1002/hyp.7990.

Ergil, M. E. (2000). "The salination problem of the Guzelyurt aquifer, Cyprus". In: *Water Research* 34.4, pp. 1201–1214.

FISRWG (1998). *Stream Corridor Restoration: Principles, Processes, and Practices*. GPO Item No. 0120-A. Federal Interagency Stream Restoration Working Group (FISRWG). United States Department of Agriculture.

Fleckenstein, Jan H., Richard G. Niswonger, and Graham E. Fogg (2006). "River-Aquifer Interactions, Geologic Heterogeneity, and Low-Flow Management". In: *Groundwater* 44.9, pp. 837–852.

Foley, Jonathan A., Ruth DeFries, Gregory P. Asner, Carol Barford, Gordon Bonan, Stephen R. Carpenter, F. Stuart Chapin, Michael T. Coe, Gretchen C. Daily, Holly K. Gibbs, Joseph H. Helkowski, Tracey Holloway, Erica A. Howard, Christo-

pher J. Kucharik, Chad Monfreda, Jonathan A. Patz, I. Colin Prentice, Navin Ramankutty, and Peter K. Snyder (2005). "Global Consequences of Land Use". In: *Science* 309.5734, pp. 570–574.

Freeze, R. A. and J. A. Cherry (1979). *Groundwater*. Englewoods Cliffs, NJ.: Prentice-Hall, Inc., 604p.

Gill, S. E., J. F. Handley, A. R. Ennos, S. Pauleit, N. Theuray, and S. J. Lindley (2008). "Characterising the urban environment of UK cities and towns: a template for landscape planning". In: *Landscape and Urban Planning* 87.3, pp. 210–222.

Gómez, J. D., J. A. López, and E. Garrido (2003). "The state of seawater intrusion in Spain". In: *Coastal Aquifers Intrusion Technology: Mediterranean Countries*, pp. 169–186.

Haase, Dagmar (2009). "Effects of urbanisation on the water balance – A long-term trajectory". In: *Environmental Impact Assessment Review* 29 (4), pp. 211–219. DOI: 10.1016/j.eiar.2009.01.002.

Harbaugh, A. W., E. R Banta, M. C Hill, and M. G. McDonald (2000). *MODFLOW-2000, The U.S Geological Survey Modular Ground-Water Model - User Guide to Modularization Concepts and the Ground-Water Flow Process*. USGS Publications Warehouse.

Harbaugh, A.W. (2005). *MODFLOW-2005, the US Geological Survey Modular Ground - Water Model the Ground-Water Flow Process*. Tech. rep. 6-A16. US Geological Survey Techniques and Methods.

Hargreaves, George H. and Zohrab A. Samani (1982). "Estimating Potential Evapotranspiration". In: *Journal of the Irrigation and Drainage Division* 108.3, pp. 225–230.

Healy, R. and P. Cook (2002). "Using groundwater levels to estimate recharge". In: *Hydrogeology Journal* 10, pp. 91–109.

Heredia, J., J.M. Murillo, J.L. García-Aróstegui, J.C. Rubio, and J.A. López-Geta (2003). "Influencia antrópica en un acuífero costero. Consideraciones sobre la gestión hídrica del acuífero Motril-Salobreña (España). (Anthropogenic influence on a coastal aqufer. Considerations on the hydraulic mnagement of the Motril-Salobreña aquifer.)" In: *Revista Latino-Americana de Hidrogeología* 3, pp. 73–83.

Hiscock, K. (2005). *Hydrogeology: principles and practice*. Blackwell Publishing Ltd.

Ibánez, S. (2005). *Comparación de la aplicación de distintos modelos matemáticos sobre acuíferos costeros detríticos.* PhD thesis. University of Granada, Spain.

IGME (1999). *Plan de Integración de los recursos hídricos subterráneos en los sistemas de abastecimiento público de Andalucía. Sector de acuíferos en relación con el abastecimiento de los núcleos situados en la cuenca del Guadalfeo y sectores costeros adyacentes (Almuñécar, Albuñol y Castell de Ferro) Granada. Actualización del conocimiento hidrogeológico de la unidad 06.21. Motril-Salobreña y Modelización matemática del acuífero. Tomo de memoria.* www.igme.es. Granada.

IGME (2000). *Actualización del conocimiento hidrogeológico de la U.H. 06.21 y modelo matemático del acuífero (Hydrogeologic studies and mathematical model of H.U. 06.21, Motril-Salobreña). Documento 15.1: Memoria. Documento 15.2: Anexos.* www.igme.es. Instituto Geológico y Minero de España (The geological institute of Spain).

IGN. *National Plan of Areal Ortophotography (NPAO) Digital terrain model (DTM), ETRS89, UTM zone 30.* Instituto Geograáfico Nacional de España(IGN).

IGN (2006). *Taxonomically generalized map of cartographic soils. 1:1.000.000.* Spanish National Geographic Institute (IGN).

Inman-Bamber, N.G. and M.G. McGlinchey (2003). "Crop coefficients and water-use estimates for sugarcane based on long-term Bowen ratio energy balance measurements". In: *Field Crops Research* 83.2, pp. 125–138.

ITGE (1988). "Estudio de viabilidad de la ampliación de la zona regable de Motril-Salobreña hasta la cota 300. Investigación hidrogeológica para apoyo a la gestión hidrológica en la cuenca del río Guadalfeo (Cuenca Sur España, Granda)." In:

Kemper, K. E. (2004). "Groundwater—from development to management". In: *Hydrogeology Journal* 12.1, pp. 3–5.

Kouzana, L., A. B. Mammou, and M. S. Felfoul (2009). "Seawater intrusion and associated processes: Case of the Korba aquifer (Cap-Bon, Tunisia)". In: *Comptes Rendus Geoscience* 341.1, pp. 21–35.

Krause, Stefan, Jörg Jacobs, and Axel Bronstert (2007). "Modelling the impacts of land-use and drainage density on the water balance of a lowland-floodplain landscape in northeast Germany". In: *Ecological Modelling.*

Lambin, Eric F. et al. (2001). "The causes of land-use and land-cover change: moving beyond the myths". In: *Global Environmental Change* 11.4, pp. 261–269.

López, D. Andrés Maldonado (2009). "El Delta Del Guadalfeo". In: *XXVII Semana De Estudios Del Mar*. Asoció de Estudios Del Mar (Asemar) Ente Público Puertos Del Estado, pp. 188–212.

Macaulay, Scott and Ian Mullen (2007). "Predicting salinity impacts of land-use change: Groundwater modelling with airborne electromagnetics and field data, SE Queensland, Australia". In: *International Journal of Applied Earth Observation and Geoinformation* 9, pp. 124–129.

Monteith, J. L. (1965). "Evaporation and environment". In: *Symposia of the Society for Experimental Biology* 19, pp. 205–234.

Moravejalahkami, B., B. Mostafazadeh-Fard, M. Heidarpour, and F. Abbasi (2009). "Furrow infiltration and roughness prediction for different furrow inflow hydrographs using a zero-inertia model with a multilevel calibration approach". In: *Biosystems Engineering* 103.3, pp. 374–381.

Mundy, G. N., K. J. Nexhip, N. R. Austin, and M. D. Collins (2003). "The influence of cutting and grazing on phosphorus and nitrogen in irrigation runoff from perennial pasture". In: *Australian Journal of Soil Research* 41, pp. 675–685.

Niswonger, Richard G. and David E. Prudic (2005). *Documentation of the Streamflow-Routing (SFR2) Package to Include Unsaturated Flow Beneath Streams - A Modification to SFR1*. Tech. rep. US Department of the Interior, US Geological Survey.

OCAM (2008). "Distribución mensual media de las dotaciones de riego (m3/ha/ano) para los cultivos de la Vega de Motril-Salobreña (valores orientativos)". In:

Pleguezuelo, Carmen R. R., Víctor H. D. Zuazo, José R. F. Martínez, José L. M. Fernández, and Dionisio F. Tarfifa (2011). "Monitoring the pollution risk and water use in orchard terraces with mango and cherimoya trees by drainage lysimeters". In: *Irrigation Drainage System* 25, pp. 61–79.

Ramankutty, Navin and Jonathan A. Foley (1999). "Estimating historical changes in global land cover: Croplands from 1700 to 1992". In: *Global Biogeochemical Cycles* 13.4, pp. 997–1027.

Roberts, Mike (2012). *Conversion from Flood to Sprinkler - Water Supply Impacts.* Presentation, Department of Natural Resources and Conservation, Water Management Bureau.

Rosegrant, Mark W., Ximing Cai, and Sarah A. Cline (2002). *Global Water Outlook to 2025.* Tech. rep. IFPRI-2020 Vision/International Water Management Institute.

Schofield, N. J. and J. K. Ruprecht (1989). "Regional analysis of stream salinisation in south-west Western Australia". In: *Journal of Hydrology* 112, pp. 19–39.

Shock, C. C. and T. Welch (2013). *Drip Irrigation: An Introduction.* EM8782. Origon State University - Malheur Extension Office.

Steduto, Pasquale, Theodore C. Hsiao, Elias Fereres, and Dirk Raes (2012). *Crop Yield response to water.* Tech. rep. Rome: Food and Agriculture Organization of the United Nations.

Switzman, Harris, Paulin Coulibaly, and Zafar Adeel (2015). "Modeling the impacts of dryland agricultural reclamation on groundwater resources in Northern Egypt using sparse data". In: *Journal of Hydrology* 520, pp. 420–438.

Syvitski, James P. M., Albert J. Kettner, Irina Overeem, Eric W. H. Hutton, Mark T. Hannon, G. Robert Brakenridge, John Day, Charles Vorosmarty, Yoshiki Saito, Liviu Giosan, and Robert J. Nicholls (2009). "Sinking deltas due to human activities". In: *Nature Geoscience* 2.10, 681–686.

Thorburn, P.J., J.S Biggs, S.J. Attard, and J. Kemei (2011). "Environmental impacts of irrigated sugarcane production: Nitrogen lost through runoff and leaching". In: *Agriculture, Ecosystems and Environment.*

Thornthwaite, C. W. (1948). "An Approach toward a Rational Classification of Climate". In: *Geographical Review* 38.1, pp. 55–94.

Watanabe, Kota, Takashi Yamamoto, Takashi Yamada, Tetsuo Sakuratani, Eiji Nawata, Chairat Noichana, Akadet Sributta, and Hirokazu Higuchi (2004). "Changes in seasonal evapotranspiration, soil water content, and crop coefficients in sugarcane, cassava, and maize fields in Northeast Thailand". In: *Agricultural Water Management* 67.2, pp. 133–143.

Weather Undergound (2015). *.* URL: www.wunderground.com.

Windfinder (2015). *Annual average wind speed in Motril.* URL: www.windfinder.com.

Xu, Xu, Guanhua Huang, Zhongyi Qu, and Luis S. Pereira (2010). "Assessing the groundwater dynamics and impacts of water saving in the Hetao Irrigation District, Yellow River basin". In: *Agricultural Water Management* 98, pp. 301–313.

Zhang, H. and K.M. Hiscock (2010). "Modelling the impact of forest cover on groundwater resources: A case study of the Sherwood Sandstone aquifer in the East Midlands, UK". In: *Journal of Hydrology*.

APPENDIX: AERIAL IMAGES OF
MOTRIL-SALOBREÑA WITH LAND USE MAPPING

1956

Land uses

- No land use
- Urban areas
- Greenhouses
- Subtropical trees
- Vegetables
- Sugarcane
- Wetlands

RM_PRETEL-1956H1055_1

Value

High : 255

Low : 0

N

Kilometers
0 .5 1 2 3 4

1974

Land uses

- No land use
- Urban areas
- Greenhouses
- Subtropical trees
- Vegetables
- Sugarcane
- Wetlands

Kilometers

0   .5   1   2   3   4

N

Kilometers
0 .5 1 2 3 4

N

1998

Land uses

- No land use
- Urban areas
- Greenhouses
- Subtropical trees
- Vegetables
- Sugarcane
- Wetlands

2004

Land uses

- No land use
- Urban areas
- Greenhouses
- Subtropical trees
- Vegetables
- Sugarcane
- Wetlands

N

Kilometers
0 .5 1 2 3 4

2007

Land uses

- No land use
- Urban areas
- Greenhouses
- Subtropical trees
- Vegetables
- Wetlands

446000 448000 450000 452000 454000 456000 458000 460000

4070000 4068000 4066000 4064000 4062000

Kilometers
0 .5 1 2 3 4

N

2012

Land uses

- No land use
- Urban areas
- Greenhouses
- Subtropical trees
- Vegetables
- Wetlands

N

Kilometers

0 .5 1 2 3 4